Report Title: Feasibility for alkali-activation of a Sewage Sludge Ash (SSA)

Authors: João Castro-Gomes[1], Naim Sedira[2], and Erick Grünhäuser Soares[3].

Summary:
The feasibility for alkali-activation of a Sewage Sludge Ash (SSA) was carried on. The study comprised alkali-activation and Portland cement hydration. A co-utilization approach for combining SSA with other industrial waste (glass waste (GW) and grounded blast furnace slag (GBFS)) was adopted. The study comprises the following: the setting time, workability (Spread test), efflorescence phenomena, compressive strength, TG-DTG, FTIR, SEM-EDS and MIP analysis.

Local: University of Beira Interior, Centre of Materials and Building Technologies
Date: March 2022

Confidentiality: Public

Report Contents:

[1] Full Professor (castro.gomes@ubi.pt)
[2] Postdoc Researcher
[3] PhD student

1 List of experimental tests

The list of chemical and physical characterization tests is exhibited in Table 1.

Table 1. Chemical and physical characterization tests.

Test
Chemical composition (SEM-EDX)
Particle size reduction
Bulk density
Specific surface area
Loss on ignition
Mineralogical characterization (XRD)
Chemical bonding through Fourier Transform Infrared Spectroscopy (FT-IR)
Structural bonding by thermogravimetric analysis (TG-DTG)

2 Materials

Incinerated Sewage Sludge Ash (SSA) was derived in the spherical shape of particle sizes between 3 to 4 mm from a local municipality. Before being used, the SSA was powdered using a Vibratory Disc Mill RS 300 Retch for 2 min using reverse function aiming to reduce its particles medium diameter. After milling, the SSA powder was sieved below 125 μm sieve mesh.

Ground Granulated Blast Furnace Slag (GBFS) was supplied, in fine powder, by a steel company, and it was used as it was received.

Glass Waste (WG) was obtained by collecting flint glass bottles from garbage; washing them in tap water to clean and remove the paper labels at the external glass surface. Afterwards, it was ground into a ball mill grinder.

The SECIL cement company provided Portland cement (PC) containing limestone under CEM II/B-L 32.5N.

River sand (RS) used as fine aggregate was provided by Tabal-Sepor Areias e Argamassas LDA and before being used, it was passed through a 4 mm sieve.

2.1 Chemical composition (SEM-EDX) and physical parameters of raw materials

The chemical composition of the raw materials was obtained using a scanning electron microscope (SEM-EDS) Hitachi S-4800 coupled with an EDX detector in Optical Centre, University of Beira Interior, Portugal.

Excluding Oxygen (O), the SSA used in this study is mainly composed of Calcium (Ca), Silica (Si) and Phosphorus (P). In contrast, GBFS is essentially composed of Ca, Si and Aluminium (Al), and PC is primarily composed of Ca, Si, and Iron (Fe). The elemental composition is detailed in Table 2.

Table 2. Chemical composition of the materials (wt.%).

Chemical composition (wt. %)	O	Al	Si	Ti	S	K	Ca	Fe	Mg	Na	P	Cl
SSA	37.6	2.38	6.23	0.44	1.15	1.0	35.46	4.73	4.2	1.0	5.3	0.4
GBFS	37.7	3.97	15.3	0.21	0.49	0.4	33.47	0.27	-	-	-	-
WG	45.1	1.37	31.75	-	-	0.62	8.51	1.14	-	10.5	-	-
PC	33.2	1.48	5.20	-	1.38	-	55.72	1.81	1.3	-	-	-

The bulk powder density was determined using a gas displacement pycnometer (model. AccuPyc1340, Micromeritics, Norcross, Georgia apparatus). The SSA bulk density corresponds to 2.9 g/cm^3, while GBFS and PC hold 3.10 and 3.01 g/cm^3, respectively.

Blaine fineness of the different powders was determined according to EN 196-6, using Blaine air permeability (model. ACMEL LABO BSA1 apparatus). The specific surface area of SSA, GBFS, WG and PC corresponds, respectively, to 6264, 4997, 2779, and 3456 cm^2/g. The Blaine specific area of SSA is quite high, which may be related to the fineness and the morphological irregularities of the SSA grains. Loss on ignition (LOI) of SSA was obtained by TG-DTG analysis, which was carried out on an SDT Q-50 (TA Instrument). This was performed in the ambient temperature range to 1000 ˚C, at a heating rate of 20 ˚C/min, using Nitrogen as the purge gas and platinum crucibles. The tested material consists of about 5 mg of sieved SSA with a diameter of less than 63 μm after sieving. The LOI of SSA, GBFS, WG and PC correspond to 16.86, 3.719, 2.0 and 11.20 wt. %, respectively.

2.2 TG-DTG curves, particle shape and mineralogical characterization (XRD) of SSA

The TG-DTG curves are exhibited in Figure 1. The DTG curves are related to Sewage Sludge Ash (SSA). It shows that SSA lost about 17% of its total weight during the heating analysis. The curve shows one single stage of weight loss of about 11% between 520 ºC and 720 ºC. This mass loss can be attributed to the decomposition of weakly crystalline calcite ($CaCO_3$). From 20 ºC to 520 ºC, the DTG curves show a weight loss of around 4%, which is possibly related to loss of free water (between 20 and 100 ºC) and dehydration of limited amounts of Mg $(OH)_2$ and Ca$(OH)_2$ (between 300 to 450 ºC). Above 720 ºC and up to 950ºC, the weight loss is less than 1% which can be related to the effect of sound crystalline calcium carbonate ($CaCO_3$) decomposition.

Universidade da Beira Interior | Faculdade de Engenharia
Calçada Fonte do Lameiro
6201-001 Covilhã | PORTUGAL

Tel.: +351 275 329 722 | E-mail: deca@ubi.pt
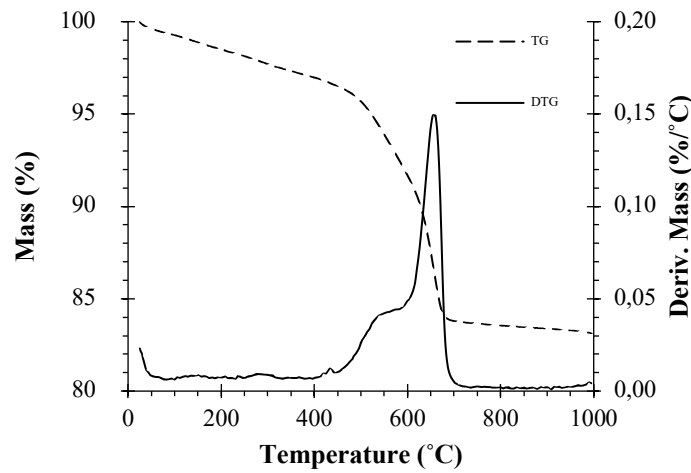
www.ubi.pt

3/53

Figure 1. TG and DTG curves of SSA.

Regarding the shape of SSA, it presents irregular grains, as shown in Figure 2 (SEM-EDS of SSA). It is also shown that it seems to be an aggregation of small particles with irregular shapes.
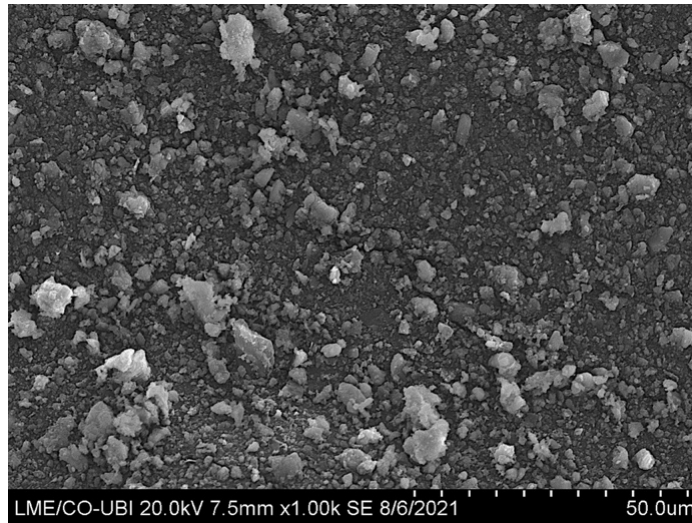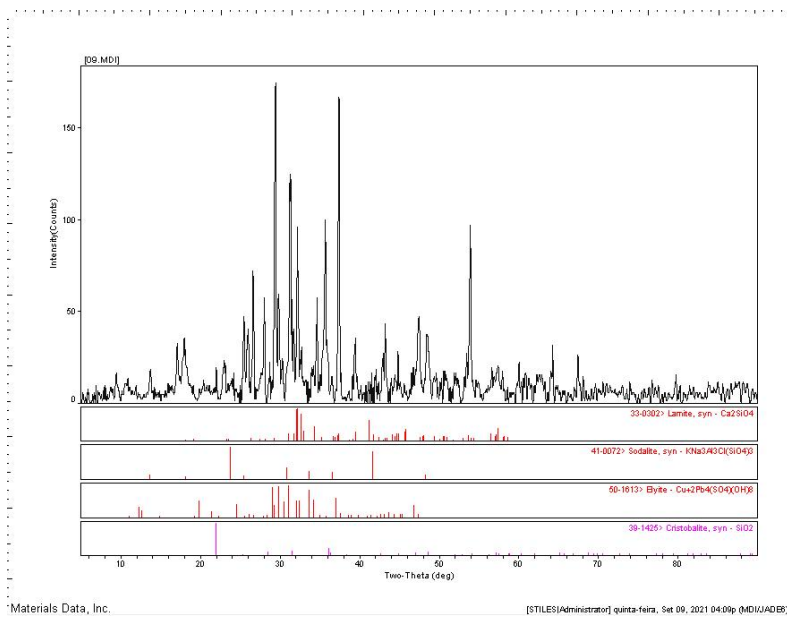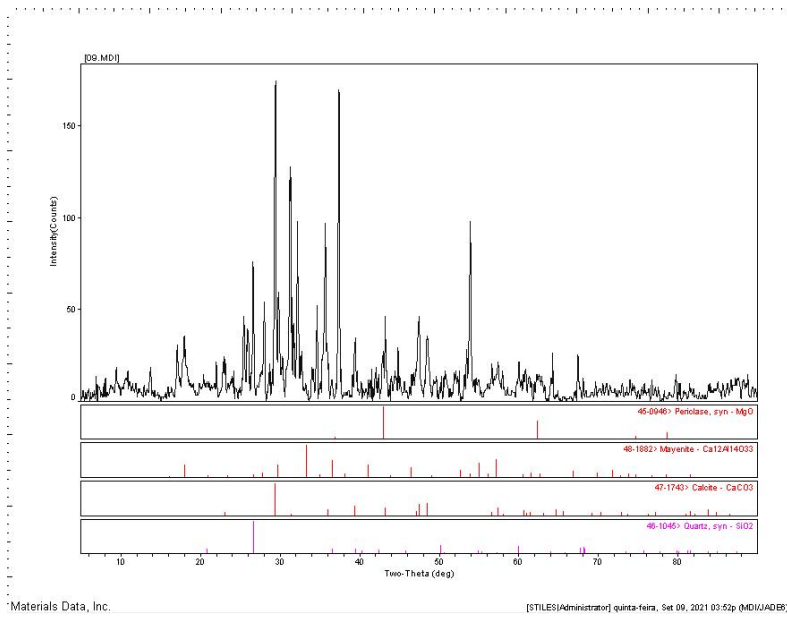

Figure 2. SEM-EDS of SSA

As shown in Figure 3, SSA is a material made of several crystallized minerals and a vitreous phase. Thus, a wide and diffusive reflection in the interval of 05-90 angles 2θ may be observed.

The principal crystallized minerals noticed are Calcite (PDF# 45-0946), Periclase (45-0946), Lamite (PDF#33-0302), Quartz (PDF# 46-1045), and Anatase (PDF# 21-1272).

Universidade da Beira Interior | Faculdade de Engenharia
Calçada Fonte do Lameiro
6201-001 Covilhã | PORTUGAL

Tel.: +351 275 329 722 | E-mail: deca@ubi.pt

www.ubi.pt

4/53

Universidade da Beira Interior | Faculdade de Engenharia
Calçada Fonte do Lameiro
6201-001 Covilhã | PORTUGAL

Tel.: +351 275 329 722 | E-mail: deca@ubi.pt
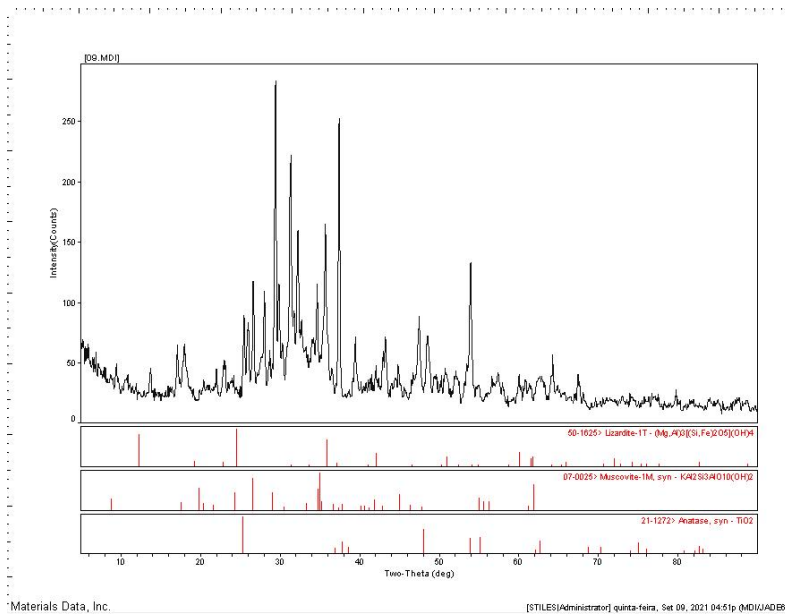
www.ubi.pt

5/53

Figure 3. XRD analysis of SSA identified crystallized minerals.
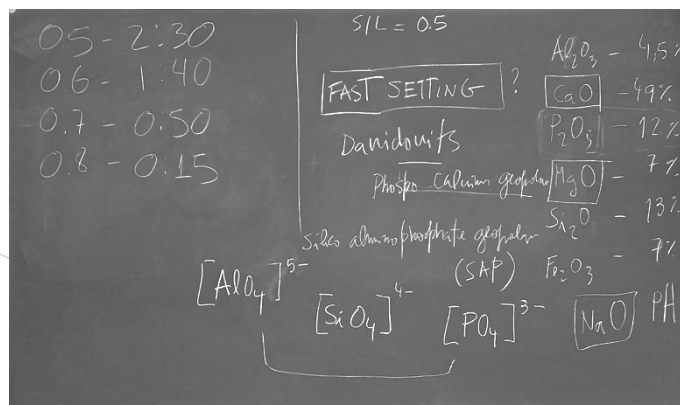
3 Methods

3.1 Preliminary study and mixture design

Although the group experience laboratory work of alkali-activated mortars, some unexpected results were observed during the preliminary studies regarding setting time, workability, and efflorescence phenomena. Thereby leading to the need to verify and understand the behaviour of the SSA-alkali-activated mortars (SSA-AAM).

For this purpose, a brief literature research was done on the (silico-aluminophosphate) SAP gels [1][2] due to the chemistry composition of SSA. Besides, 28 mixtures were done aiming to solve such unexpected results.

Figure 4 presents some of the blackboard schemes made.

a)

b)

Universidade da Beira Interior | Faculdade de Engenharia
Calçada Fonte do Lameiro
6201-001 Covilhã | PORTUGAL

Tel.: +351 275 329 722 | E-mail: deca@ubi.pt

www.ubi.pt

6/53
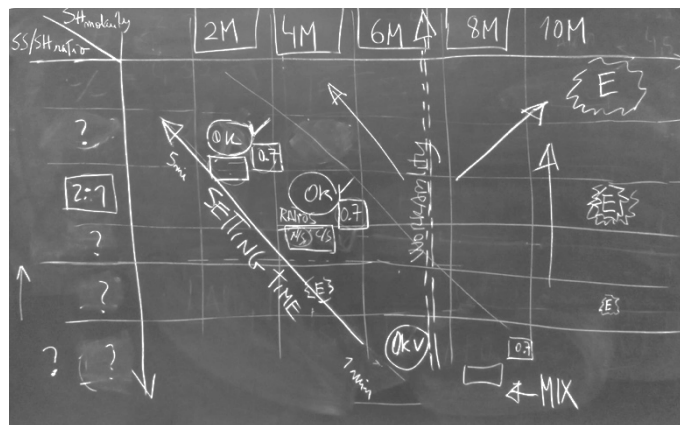
c)

Figure 4. Blackboard schemes for the preliminary study and controlling efflorescence (C-MADE Lab).

3.1.1 Proposed mortars at the preliminary study

Different mortar mixtures embodying SSA were designed to compare the influence of different activator solutions, activators molarity and liquid to solid ratio on SSA-alkali-activated mortars (SSA-AAM). The mortars were prepared using sand to precursor at a ratio of 3/1 as a fixed parameter.

The current study used two alkaline activators: sodium silicate and sodium hydroxide (NaOH). A sodium silicate, commercially known as D40, with a modulus of silicate (SiO_2/Na_2O) equal to 3.23, was supplied by QUIMIALMEL, Portugal. Besides, its weight percentual (wt.%) chemical composition is 8.60 % of Na_2O, 27.79 % of SiO_2, 63.19 % of H_2O, and 0.4 % of Al_2O_3. DOS SANTOS, Lda Portugal, supplied sodium hydroxide in flakes of 98,6 % purity. The sodium hydroxide solution was prepared by dissolving NaOH pellets in distilled water to provide different molarity, preserved in room temperature conditions for 24 h before cooling down.

The 28 different mortar mixtures prepared in the study are shown in Table 3.

Universidade da Beira Interior | Faculdade de Engenharia
Calçada Fonte do Lameiro
6201-001 Covilhã | PORTUGAL

Tel.: +351 275 329 722 | E-mail: deca@ubi.pt

www.ubi.pt

7/53

Table 3. Mixture recipes.

Mix Label	Solution	S/L	SS/SH	M	Sand:Precursor	SSA	PC	GW	GBFS
SSA1.2-1/0-0-Air	Activator	1.20	1/0	0	3:1	100%	0%	0%	0%
SSA1.2-5/1-10-Air	Activator	1.20	5/1	10	3:1	100%	0%	0%	0%
SSA1.2-0/1-4-Air	Activator	1.20	0/1	4	3:1	100%	0%	0%	0%
SSA1.2-5/1-4-Air	Activator	1.20	5/1	4	3:1	100%	0%	0%	0%
SSA0.7-1/2-4-Air	Activator	0.70	1/2	4	3:1	100%	0%	0%	0%
SSA0.6-1/2-4-Air	Activator	0.60	1/2	4	3:1	100%	0%	0%	0%
SSA0.5-1/2-4-Air	Activator	0.50	1/2	4	3:1	100%	0%	0%	0%
SSA0.5-1/2-10-Air	Activator	0.50	1/2	10	3:1	100%	0%	0%	0%
SSA0.7-1/2-10-Air	Activator	0.70	1/2	10	3:1	100%	0%	0%	0%
SSA0.6-1/2-10-Air	Activator	0.60	1/2	10	3:1	100%	0%	0%	0%
SSA1.2-1/2-4-Air	Activator	1.20	1/2	4	3:1	100%	0%	0%	0%
SSA0.9-1/2-4-Air	Activator	0.90	1/2	4	3:1	100%	0%	0%	0%
SSA0.8-19/1-4-Air	Activator	0.80	19/1	4	3:1	100%	0%	0%	0%
SSA0.8-9/1-4-Air	Activator	0.80	9/1	4	3:1	100%	0%	0%	0%
SSA0.9-19/1-4-Air	Activator	0.90	19/1	4	3:1	100%	0%	0%	0%
SSA0.9-9/1-4-Air	Activator	0.90	9/1	4	3:1	100%	0%	0%	0%
SSA1.1-0/1-4-Air	Activator	1.10	0/1	4	3:1	75%	0%	25%	0%
SSA1.1-0/1-10-Air	Activator	1.10	0/1	10	3:1	75%	0%	25%	0%
SSA0.9-0/1-4-Air	Activator	0.90	0/1	4	3:1	75%	0%	25%	0%
SSA0.9-0/1-10-Air	Activator	0.90	0/1	10	3:1	75%	0%	25%	0%
SSA1.2-5/1-4-60˚C	Activator	1.20	5/1	4	3:1	100%	0%	0%	0%
SSA1.2-5/1-10-60˚C	Activator	1.20	5/1	10	3:1	100%	0%	0%	0%
SSA1.1-0/1-4-Air	Activator	1.10	0/1	4	3:1	90%	0%	0%	10%
SSA1.2-0/1-4-Air	Activator	1.20	0/1	4	3:1	80%	0%	0%	20%
SSA0.6-SSA1-PC0-Air	Water	0.60	-	-	3:1	100%	0%	0%	0%
SSA0.6-SSA0.25-PC0.75-Air	Water	0.60	-	-	3:1	25%	75%	0%	0%
SSA0.65-SSA0.25-PC0.75-Air	Water	0.65	-	-	3:1	25%	75%	0%	0%
SSA0.55-SSA0.25-PC0.75-Air	Water	0.55	-	-	3:1	25%	75%	0%	0%

3.1.2   Setting Time

In general, the initial setting time of the SSA-AAM was unexpectedly fast; to understand the reason behind the fast initial setting time, a study about the chemical composition was carried out. Additionally, a multi-parameter preliminary study was conducted by preparing a series of mixtures with different parameters since many factors may exert

Universidade da Beira Interior | Faculdade de Engenharia
Calçada Fonte do Lameiro
6201-001 Covilhã | PORTUGAL

Tel.: +351 275 329 722 | E-mail: deca@ubi.pt

www.ubi.pt

8/53

influence on the initial setting time of SSA-AAM; namely the SSA complex chemical composition and as well as:

- The type of the alkali-activator solution;
- The Molarity of NaOH solution;
- The ratios (NaOH/Sodium silicate and Solid/ Liquid);
- The type of precursors (use of different materials);
- The curing conditions.

The samples prepared with only sodium silicate had the fastest initial setting time. However, the samples prepared with NaOH 4M presented the longest initial setting time than the other samples. Besides that, the increase in the Molarity of NaOH from 4M to 10M led to an even faster initial setting time. On the other hand, the setting time may be prolonged by increasing the liquid to solid (L/S) ratios since the samples prepared with higher solid to liquid (S/L) ratios showed the faster initial setting time, probably due to the high liquid absorption rate of SSA.

Based on the literature, the fast setting of the SSA-AAM may be due to the fineness of SSA. It may be related to the presence of soluble calcium (Ca) and aluminium (Al) in the chemical composition of SSA as precursors. Besides, the hydration rate of aluminium oxide in SSA is faster than that of calcium silicates in Ordinary Portland Cement (OPC). When SSA fineness increased to 780–1,000 m^2/kg, the initial and final setting times of SSA-based cement paste tends to be prolonged to about 3.5–5 and 7–8 h, respectively [3]. Thus, the fast initial setting time of SSA-AAM may be due to the presence of soluble aluminium in the SSA as a precursor, which tends to accelerate the geopolymerisation in the mixture at the early stage of reaction resulting in fast setting time.

Figure 5. Different solution and same liquid to solid ratio. From left to right: Sodium Hydroxide only; Sodium Silicate and Sodium Silicate; and Sodium Silicate only.

Universidade da Beira Interior | Faculdade de Engenharia
Calçada Fonte do Lameiro
6201-001 Covilhã | PORTUGAL

Tel.: +351 275 329 722 | E-mail: deca@ubi.pt
www.ubi.pt

9/53

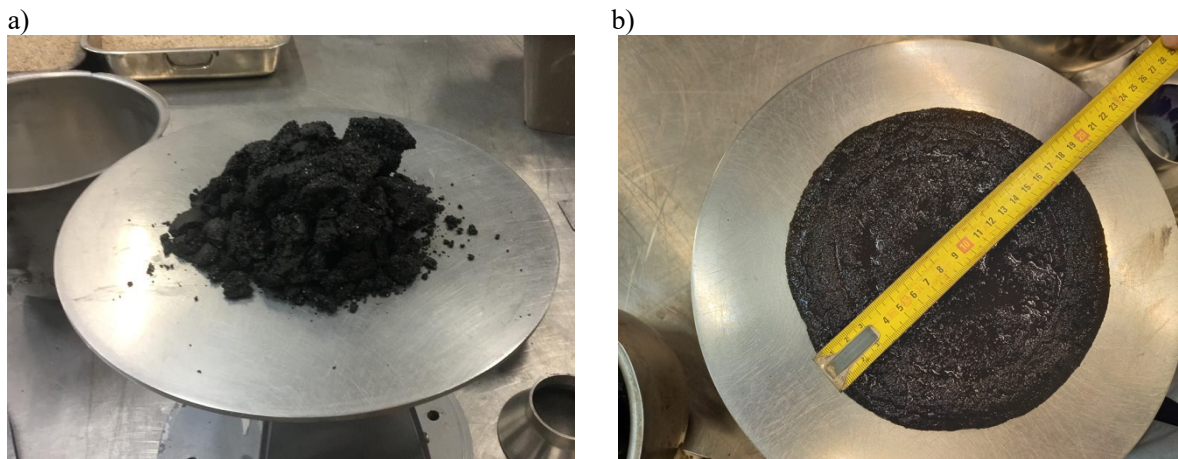Figure 6. Different liquid to solid ratio and same solution.

a)

b)

Figure 7. (a) Extremely fast setting and (b) good workability and normal setting time.

3.1.3 Efflorescence in the SSA-AAM

The mortars prepared with alkaline activator solutions (sodium hydroxide, sodium silicate, sodium hydroxide blended with sodium silicate) suffer from efflorescence phenomena. It was noticed that the formation of efflorescence in the SSA-AAM increases with the increase of the molarity of the sodium hydroxide in the mixtures. Further, the samples with a higher L/S ratio generated more efflorescence. Besides, in the same manner as for alkali-activation different factors besides SSA complex chemical composition may influence the formation of efflorescence in the SSA-AAM, such as:
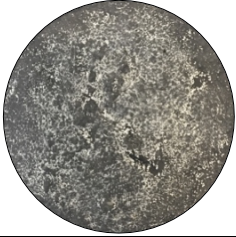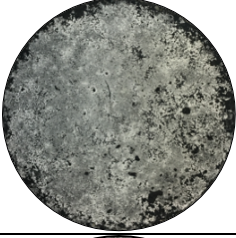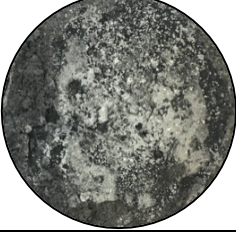
- The type of the alkali-activator solution;
- The Molarity of NaOH solution;
- The ratios (NaOH/Sodium silicate and Solid/ Liquid);
- The type of precursors (use of different materials);
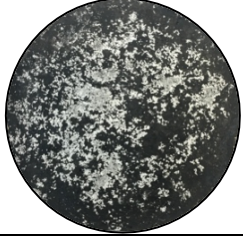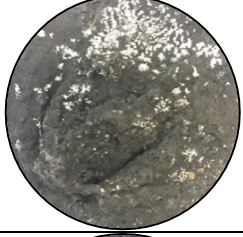- The curing conditions.

Universidade da Beira Interior | Faculdade de Engenharia
Calçada Fonte do Lameiro
6201-001 Covilhã | PORTUGAL

Tel.: +351 275 329 722 | E-mail: deca@ubi.pt
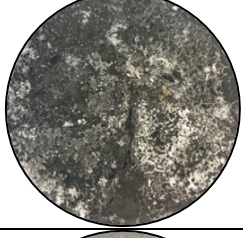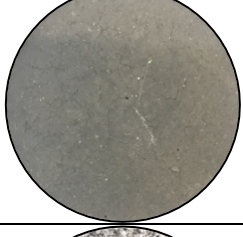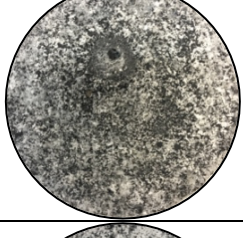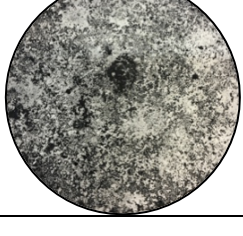
www.ubi.pt

10/53

Adjusting these parameters could help better understand efflorescence phenomena in the SSA-AAM. Although different alkaline activator solutions and NaOH concentrations were used, we noticed the efflorescence crystals in samples cured at ambient temperature. On the other hand, when the SSA-AAM specimens were cured at a temperature (60 ºC), the phenomena of efflorescence did not appear, probably due to the acceleration of the alkaline activation reactions. Since the content of free Na+ and K+ tends to react faster with the other chemical components to form reaction materials such as N-A-S-H and (N, C)-A-S-H. In addition, mixtures consumed more water to develop the reaction products, which limited the carbonation reaction. Besides, it also suffered a negative influence due to the increase of water evaporation from the specimens' surface due to the high temperature under the curing, thus decreasing the dissolution of CO_2 in H_2O.
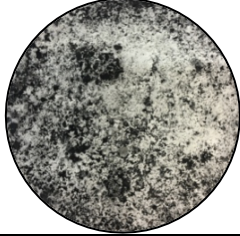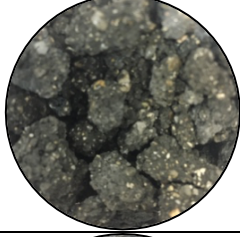
3.1.4 Summary of results observed in each mix label

The summary of the efflorescence phenomena and setting time observed in the mixture labels developed in this study is exhibited in Table 4. Besides, the best mixture labels concerning efflorescence phenomena and setting are grey.

Table 4. Mixture labels and summary of their results.
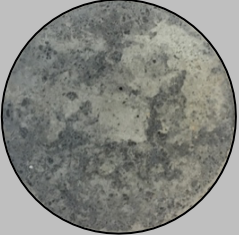
Mix Label	Setting	Efflorescence	Image
SSA1.2-1/0-0-Air	Normal	Light	
SSA1.2-5/1-10-Air	Normal	Medium	
SSA1.2-0/1-4-Air	Normal	Light	

Universidade da Beira Interior | Faculdade de Engenharia
Calçada Fonte do Lameiro
6201-001 Covilhã | PORTUGAL

Tel.: +351 275 329 722 | E-mail: deca@ubi.pt

www.ubi.pt

11/53

SSA1.2-5/1-4-Air	Normal	Medium	
SSA0.7-1/2-4-Air	Very fast	Light	
SSA0.6-1/2-4-Air	Fast	High	
SSA0.5-1/2-4-Air	Normal	Light	
SSA0.5-1/2-10-Air	Normal	Very high	
SSA0.7-1/2-10-Air	Normal	High	

Universidade da Beira Interior | Faculdade de Engenharia
Calçada Fonte do Lameiro
6201-001 Covilhã | PORTUGAL

Tel.: +351 275 329 722 | E-mail: deca@ubi.pt

www.ubi.pt

12/53

SSA0.6-1/2-10-Air	Normal	Very high	
SSA1.2-1/2-4-Air	Extremely high (no sample)	Very light	
SSA0.9-1/2-4-Air	Extremely high (no sample)	Very light	
SSA0.8-19/1-4-Air	Fast	Light	
SSA0.8-9/1-4-Air	Fast	Light	
SSA0.9-19/1-4-Air	Normal	Medium	

Universidade da Beira Interior | Faculdade de Engenharia
Calçada Fonte do Lameiro
6201-001 Covilhã | PORTUGAL

Tel.: +351 275 329 722 | E-mail: deca@ubi.pt

www.ubi.pt

13/53

SSA0.9-9/1-4-Air	Normal	Medium	
SSA1.1-0/1-4-Air	Slow	Very light	
SSA1.1-0/1-10-Air	Very fast	None	
SSA0.9-0/1-4-Air	Slow	Very light	
SSA0.9-0/1-10-Air	Fast	None	
SSA1.2-5/1-4-60˚C	Normal	None	

Universidade da Beira Interior | Faculdade de Engenharia
Calçada Fonte do Lameiro
6201-001 Covilhã | PORTUGAL

Tel.: +351 275 329 722 | E-mail: deca@ubi.pt

www.ubi.pt

14/53

SSA1.2-5/1-10-60°C	Normal	None	
SSA1.1-0/1-4-Air	Normal	Light	
SSA1.2-0/1-4-Air	Normal	Light	
SSA0.6-SSA1-PC0-Air	Slow	None	
SSA0.6-SSA0.25-PC0.75-Air	Slow	None	
SSA0.65-SSA0.25-PC0.75-Air	Slow	None	

Universidade da Beira Interior | Faculdade de Engenharia
Calçada Fonte do Lameiro
6201-001 Covilhã | PORTUGAL

Tel.: +351 275 329 722 | E-mail: deca@ubi.pt
www.ubi.pt

15/53

SSA0.55-SSA0.25-PC0.75-Air	Slow	None	

3.1.5 Conclusions of the preliminary study and mixtures design

A preliminary study was conducted to develop a mixture design with good workability and setting time allied to no efflorescence phenomena. This study found that many factors may exert influence on the SSA-AAM developed due to its complex chemical composition, such as (i) type of the alkali-activator solution; (ii) molarity of NaOH solution; (iii) ratios (NaOH/sodium silicate and Solid/ Liquid); (iv) type of precursors (use of different materials); and (v) curing conditions.

Therefore, the mixture labels suggested are SSA1.2-5/1-4-60˚C and SSA1.2-5/1-10-60˚C since these mixtures achieved normal setting time and good workability without presenting the efflorescence phenomena.

3.2 Mixtures design and preparation

The mixtures design phase aimed to study the feasibility of higher and lower NaOH molar concentration chemical activation of SSA blended with grounded granulated blast furnace slag (GGBFS). As in the preliminary phase study, the alkali-activation was obtained using NaOH and sodium silicate solutions. Besides, the mixtures design phase also aimed to obtain chemical activation of SSA with Portland cement.

3.2.1 Alkali-activated mortar

Two types of mortar were studied in this research: (a) the alkali-activated mortar prepared with different alkali-activated binders using the precursors powder (SSA and GBFS); and (b) the alkali activator solutions used were sodium silicate (D40) and sodium hydroxide (different concentration 4, 6, 8 and 10 Mole).

The mortar specimens were prepared using two binders blended with river sand. The proportion of binder/sand was 1/3. The precursors powder used in this investigation were swedge sludge ash and grounded granulated blast furnace slag. Three mixtures were designed to compare the influence of the different alkaline activators' concentrations and the liquid to solid ratios on the swedge sludge ash-based alkali-activated mortar.

The activators were used with different molar ratios. They were mixed for 5 min before mixing with the precursors to obtain the alkaline hybrid binders. The six mixtures are shown in Table (2). To improve the compressive strength results and the mechanical properties of the SSA-based alkali-activated mortars, the precursor powder was blended with 20 wt. % and 50

Universidade da Beira Interior | Faculdade de Engenharia
Calçada Fonte do Lameiro
6201-001 Covilhã | PORTUGAL

Tel.: +351 275 329 722 | E-mail: deca@ubi.pt

www.ubi.pt

16/53

wt. % of GBFS. The blended precursors were activated with different concentrations of the alkali activator solutions.

The alkali-activated mortar specimens were poured into the curing moulds. Then, the filled moulds were placed in an oven at 60 °C for 24 hours. During synthesis, to avoid water evaporation of the alkali-activated mortar, the filled moulds were wrapped with plastic film during the oven curing. After the initial 24 hours oven curing period, the specimens were de-moulded and were left to cure in laboratory condition (about 20 ºC) until the test ages (7, 14 and 28 days).

3.2.2   Cement mortar

SSA replaced the cement with the proportions 25, 50 and 75 Vt.%. The water/powder ratio was 0.50. After 7 days of curing time, the specimens were de-moulded and were left to cure in laboratory condition (about 20 ºC) until the test ages (7, 14 and 28 days).

3.2.3   Summary of the mortars produced

The summary of the mortars produced in this study is presented in Table 5 containing the volume precursors, the molarity and SS/SH, L/S. Besides, all mortar consists of a solid binder to sand at a volume ratio of 1/3.

Table 5. Mixture designs.

Mixture	Mixture Information					
	SSA (wt. %)	PC (Wt. %)	GBFS (Wt. %)	Molarity	SS/SH	L/S
SSA - 4M - 5/1 - 1.85	100	-	-	4	5/1	1.85
SSA - 6M - 5/1 - 1.85	100	-	-	6	5/1	1.85
SSA - 8M - 5/1 - 1.85	100	-	-	8	5/1	1.85
SSA - 10M - 5/1 - 1.85	100	-	-	10	5/1	1.85
SSA - 4M - 3/2 - 1.2	100	-	-	4	3/2	1.20
SSA - 6M - 3/2 - 1.2	100	-	-	6	3/2	1.20
SSA - 8M - 3/2 - 1.2	100	-	-	8	3/2	1.20
SSA - 10M - 3/2 - 1.2	100	-	-	10	3/2	1.20
80SSA20GBFS - 4M	80	-	20	4	5/1	1.85
80SSA20GBFS - 6M	80	-	20	6	5/1	1.85
80SSA20GBFS - 8M	80	-	20	8	5/1	1.85
80SSA20GBFS - 10M	80	-	20	10	5/1	1.85
50SSA50GBFS - 4M	50	-	50	4	3/2	1.50
50SSA50GBFS - 6M	50	-	50	6	3/2	1.50

Universidade da Beira Interior | Faculdade de Engenharia
Calçada Fonte do Lameiro
6201-001 Covilhã | PORTUGAL

Tel.: +351 275 329 722 | E-mail: deca@ubi.pt

www.ubi.pt

17/53

50SSA50GBFS - 8M	50	-	50	8	3/2	1.50
50SSA50GBFS - 10M	50	-	50	10	3/2	1.50
25SSA75PC	25	75	-	-	0	0.50
50SSA50PC	50	50	-	-	0	0.50
75SSA25PC	75	25	-	-	0	0.50

Figure 8. Mortars and pastes produced (C-MADE Lab).

3.3   Compressive Strength

The compressive strength tests were performed on 3000 kN electro-hydraulic mechanical testing machine "ADR Touch 3000 BS EN Compression Machine with Digital Readout and Self Centring Platens", following EN 196-1. Compressive strength data was obtained using 40 *40 *40 mm cubic size specimens

3.4   TG-DTG

Thermogravimetry and derivative thermogravimetry (TG-DTG) analysis of the specimens was carried out on a SDT Q-50 (TA Instrument). This was performed in the ambient temperature range to 1000 ˚C, at a heating rate of 20 ˚C/min, using helium as the purge gas and platinum crucibles. The tested material consists of about 5 mg of a powdered specimen with a diameter of less than 63 μm. The software Universal Analysis 2000 was used to analyze the data.
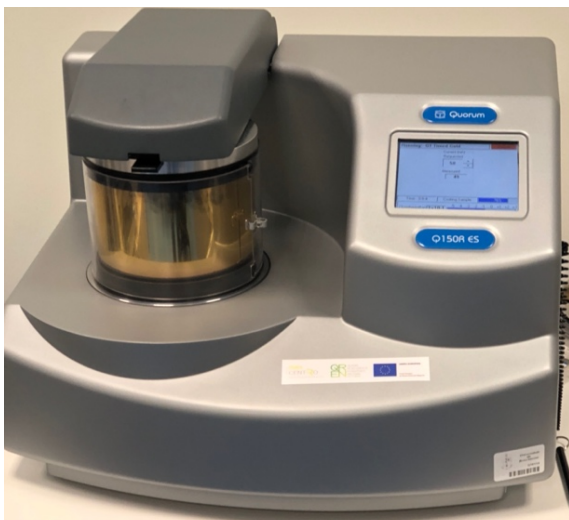
3.5   FT-IR

The Fourier transform infrared spectroscopy (FT-IR) data were recorded from 600 to 4000 cm^{-1} using Nicolet iS10 FT-IR Spectrometer (Thermo Scientific), Smart iTR accessory instrument by diamond HATR crystal. The material consists of particles passing through a 63 μm aperture sieve of powdered specimens.

Universidade da Beira Interior | Faculdade de Engenharia
Calçada Fonte do Lameiro
6201-001 Covilhã | PORTUGAL

Tel.: +351 275 329 722 | E-mail: deca@ubi.pt
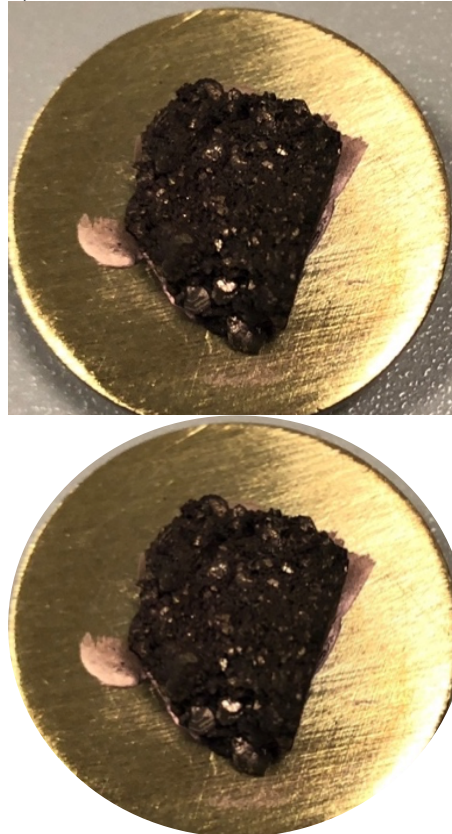
www.ubi.pt

18/53

3.6 SEM-EDX

The microstructure of the mortar was studied after 28 days of curing using a scanning electron microscope Hitachi S-4800 coupled with an EDX detector in Optical Centre, University of Beira Interior. The samples were coated with gold.
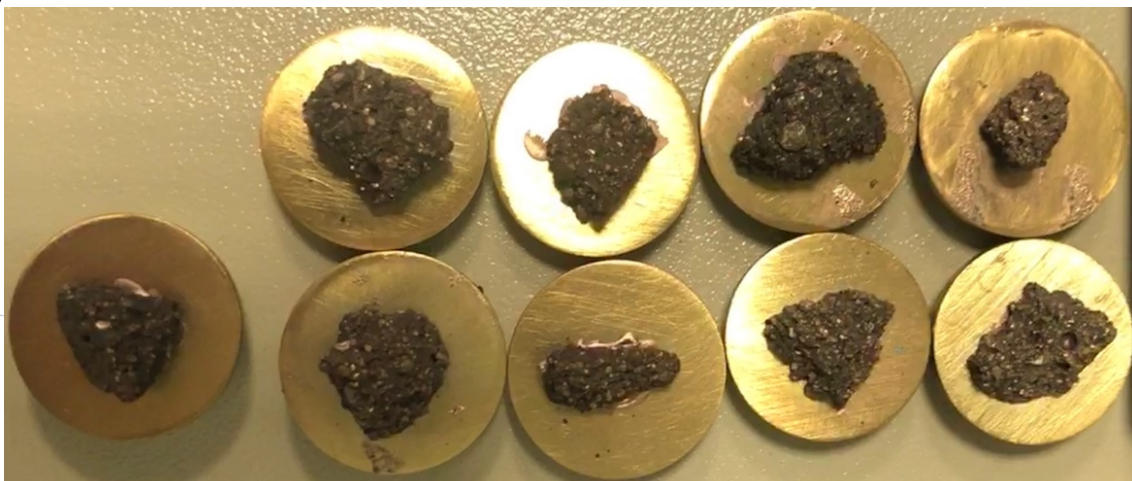
a)

b)

c)

Figure 9. (a) Rotary Coater; (b) A sample coated with gold; (c) Set of samples.

Universidade da Beira Interior | Faculdade de Engenharia
Calçada Fonte do Lameiro
6201-001 Covilhã | PORTUGAL

Tel.: +351 275 329 722 | E-mail: deca@ubi.pt

www.ubi.pt

19/53

3.7 MIP

Mercury Intrusion Porosimetry (MIP) using a Microporometrics AutoPore IV 9500 V1.07. Mercury porosimetry data is obtained by recording the volume of mercury that penetrates the porous specimen as a function of pressure. The samples left in a Glass Desiccator contain Silica gel to ensure moisture removal from the samples for 7 days.

Figure 10. Set of samples drying for MIP testing.

4 Results and Discussion

4.1 Mixtures surface efflorescence occurrence

4.1.1 Effect of the alkali activator concentration on the surface efflorescence occurrence of the SSA-alkali-activated mortar

Although every specimen produced with an L/S ratio of 1.85 and SS/SH ratio of 5 present efflorescence on the age of 28 days, those that used sodium silicate concentration equal to 4 M and 10 M exhibited much lower efflorescence on the surface than the samples prepared with sodium silicate concentration equal to 6 M and 8 M as is shown in Figure 11.

Universidade da Beira Interior | Faculdade de Engenharia
Calçada Fonte do Lameiro
6201-001 Covilhã | PORTUGAL

Tel.: +351 275 329 722 | E-mail: deca@ubi.pt
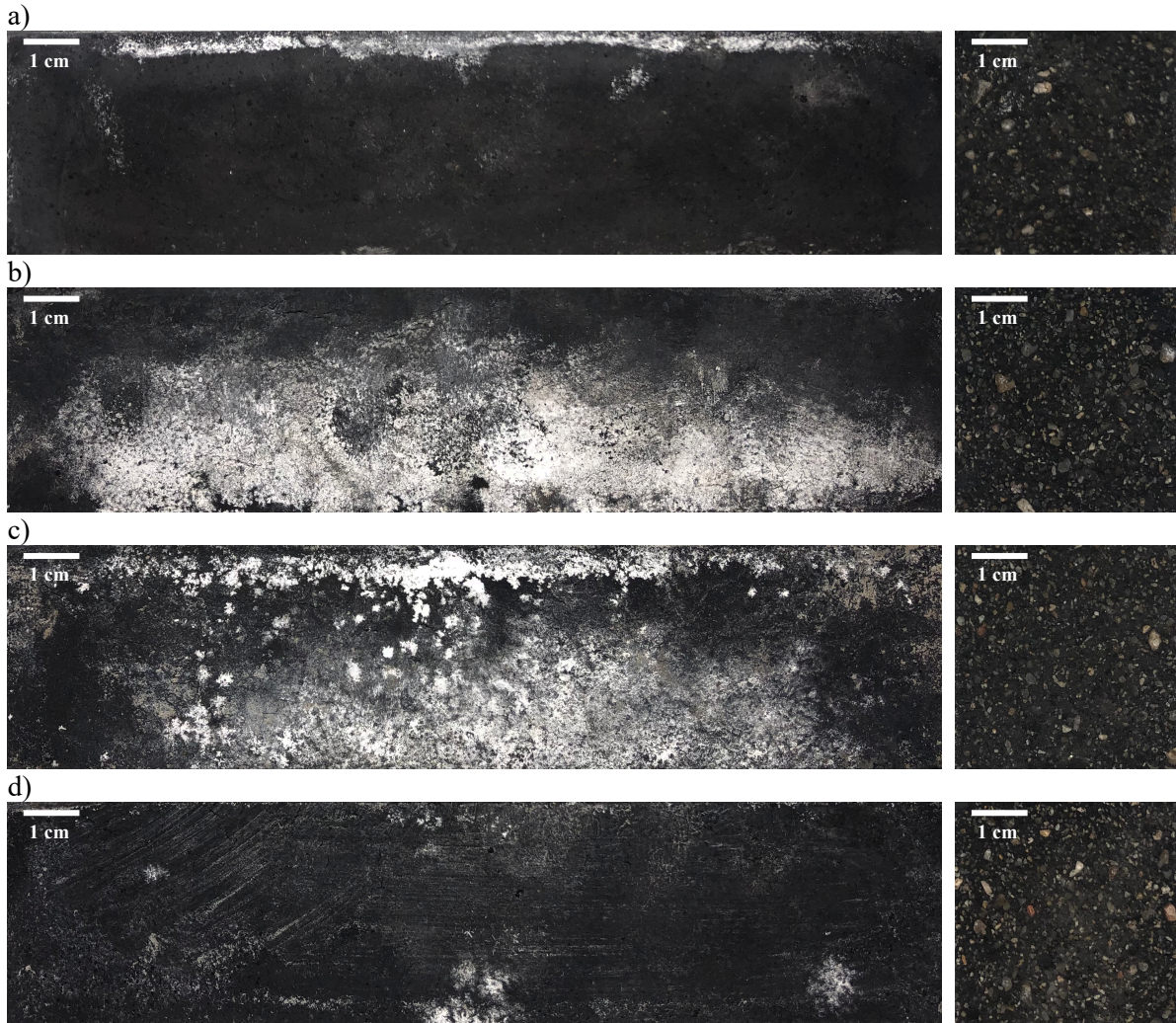
www.ubi.pt

20/53

Figure 11. Surface and cross section of SSA - 5/1 - 1.85 (a) 4M; (b) 6M; (c) 8M; and (d) 10M.

In contrast with the previous set of specimens, those produced with an L/S ratio of 1.2 and SS/SH ratio of 3/2 exhibited a slight presence of efflorescence on the age of 28 days, especially those that used sodium silicate concentration equal to 4 M and 10 M as is shown in Figure 12.
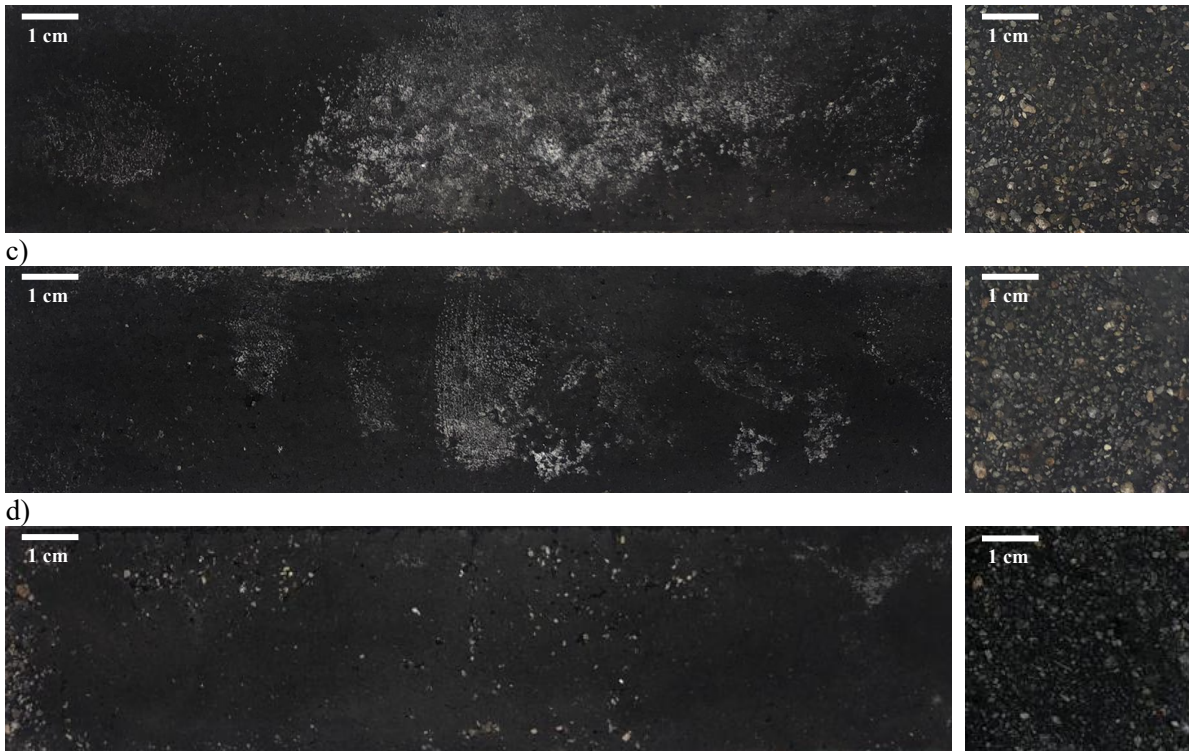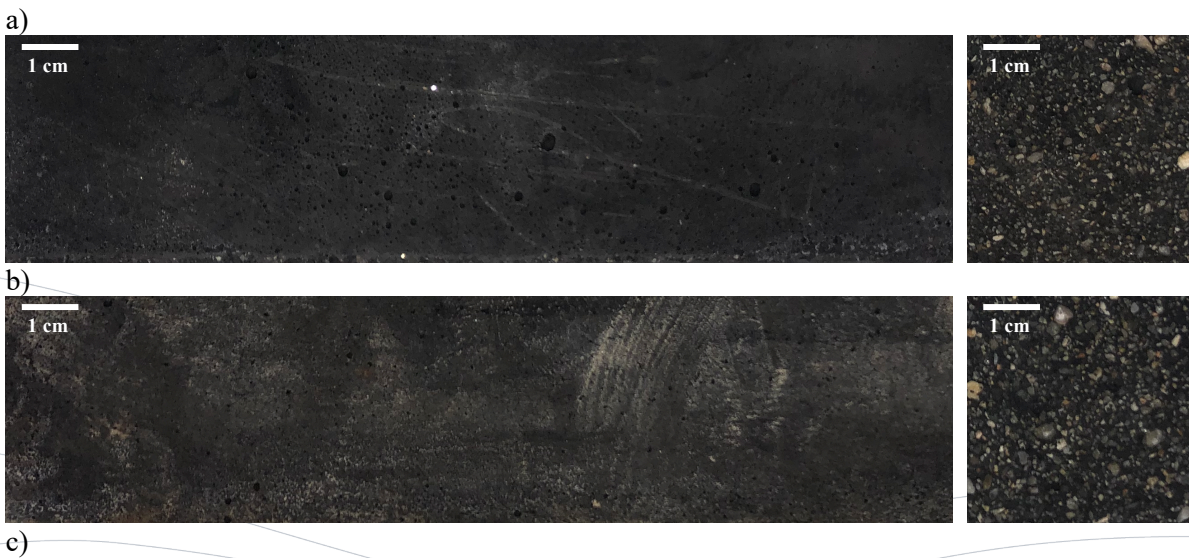
Figure 12. Surface and cross section of SSA - 3/2 - 1.2 (a) 4M ; (b) 6M; (c) 8M; and (d) 10M.

4.1.2 Effect of GBFS on the efflorescence

The specimens prepared with the blended SSA-GBFS alkali-activated binders (80 Wt. % SSA blended with 20 Wt.%) exhibited almost no efflorescence on their surface on the 28th day after being assembled, as shown in Figure 13.

Universidade da Beira Interior | Faculdade de Engenharia
Calçada Fonte do Lameiro
6201-001 Covilhã | PORTUGAL

Tel.: +351 275 329 722 | E-mail: deca@ubi.pt
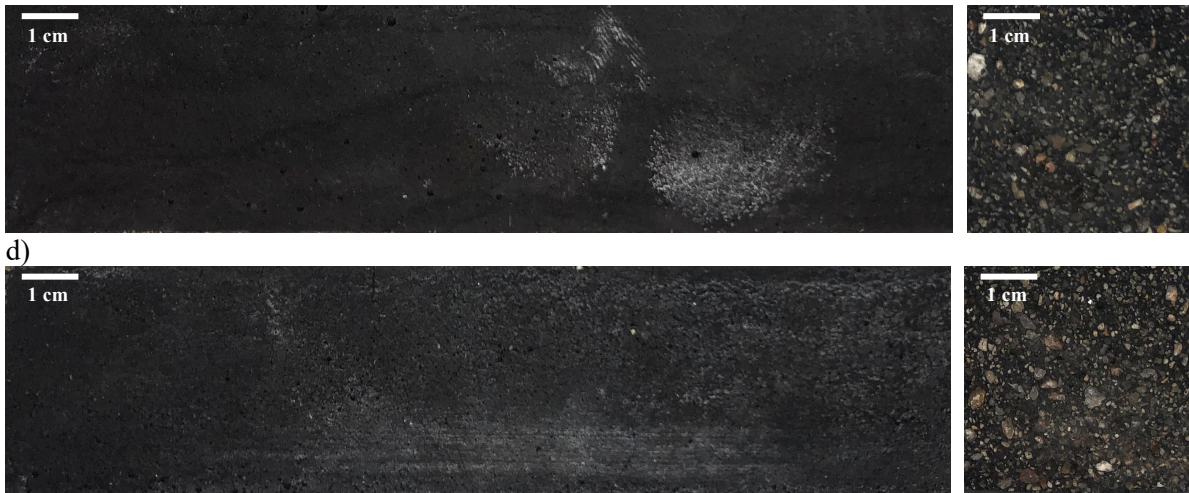
www.ubi.pt

22/53

d)

Figure 13. Surface and cross section of 80SSA20GBFS (a) 4M ; (b) 6M; (c) 8M; and (d) 10M.

The specimens prepared with the blended SSA-GBFS alkali-activated binders (50 Wt. % SSA blended with 50 Wt.%) presented no efflorescence on their surface at the age of 28 days, as exhibited in Figure 14. Besides that, the sodium hydroxide concentration affected the setting time of the alkali-activated mortar. Thereby, the setting time decreases with the increase of the sodium hydroxide concentration. Thus, the samples prepared with 4 M presented a fast-setting time which did not fill the mould, even though the moulds were submitted to vibration using a vibration concrete table. The samples prepared with 4 M shows a discontinuous sample with cavity due to the fast setting of the sample. The samples prepared with the 10 M shows a compacted structure with less visible pores.

a)

b)

c)

Universidade da Beira Interior | Faculdade de Engenharia
Calçada Fonte do Lameiro
6201-001 Covilhã | PORTUGAL

Tel.: +351 275 329 722 | E-mail: deca@ubi.pt
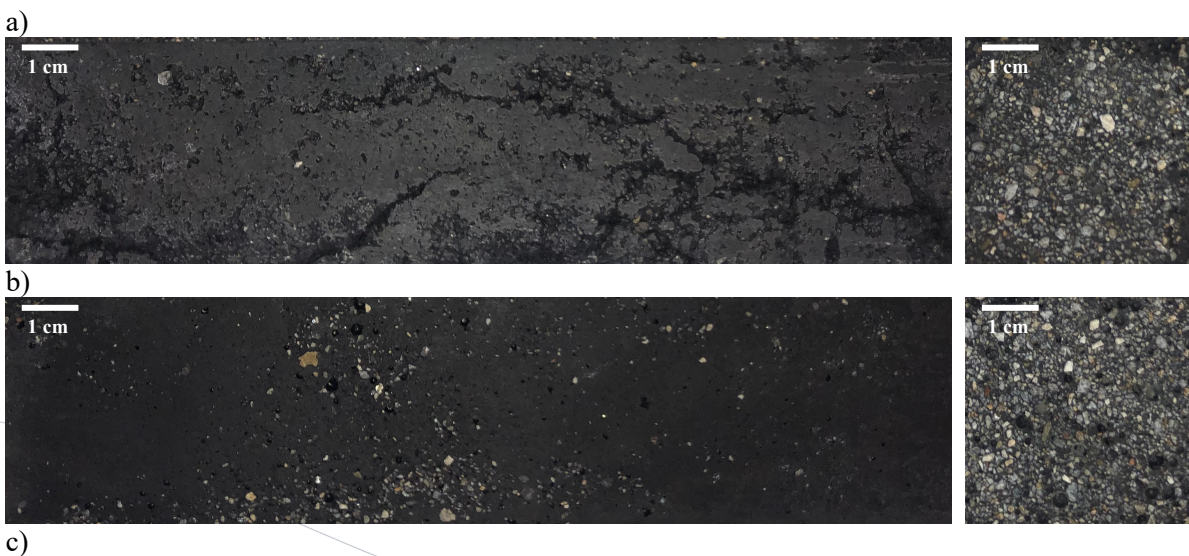
www.ubi.pt

23/53

Figure 14. Surface and cross section of 50SSA50GBFS (a) 4M; (b) 6M; (c) 8M; and (d) 10M.

Finally, as expected, the specimens that used PC in their composition did not manifest efflorescence phenomena. However, these three mixture designs presented larger pores as the SSA concentration increases, as shown in Figure 15.
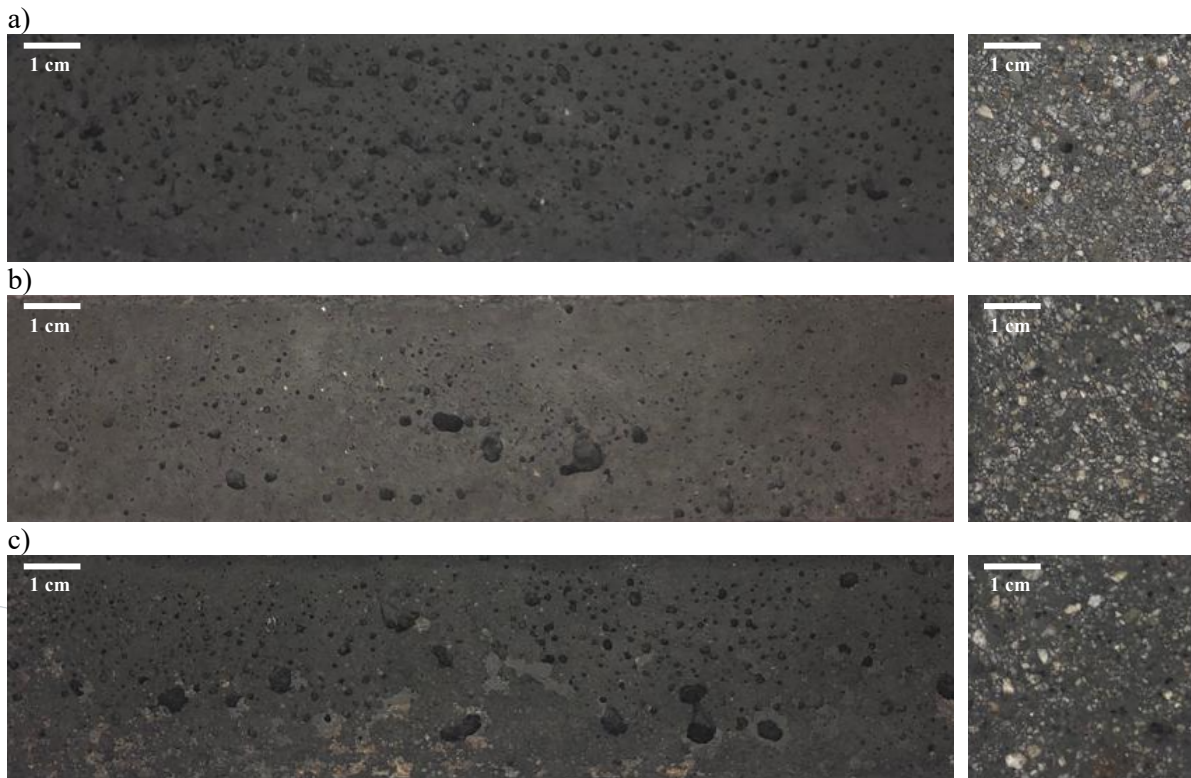

Figure 15. Surface and cross section of: (a) 25SSA75PC (b) 50SSA50PC; (c) 75SSA25PC.

Universidade da Beira Interior | Faculdade de Engenharia
Calçada Fonte do Lameiro
6201-001 Covilhã | PORTUGAL

Tel.: +351 275 329 722 | E-mail: deca@ubi.pt

www.ubi.pt

24/53

4.2 Compressive Strength

The compressive strength results are presented in Table 6 and Figure 16. The observed results along the curing time did not exhibit only enhancement in compressive strength for all mixtures. Some of them displayed loss of compressive strength as the curing time proceeded, especially the compositions of 50SSA50GBFS (from 6 to 10 M). Besides that, a similar trend was also observed in SSA - 6M - 3/2 - 1.2, 75SSA25PC, and 80SSA20GBFS - 10M, where the highest result was not found in 28 days curing age.

Table 6. Compressive strength results.

Mixture	Compressive Strength (MPa)			Standard Deviation (MPa)		
	7 days	14 days	28 days	7 days	14 days	28 days
SSA - 4M - 5/1 - 1.85	1.46	2.40	**3.27**	0.18	0.40	0.06
SSA - 6M - 5/1 - 1.85	1.57	2.77	**3.07**	0.21	0.04	0.06
SSA - 8M - 5/1 - 1.85	1.57	2.79	**3.70**	0.25	0.07	0.00
SSA - 10M - 5/1 - 1.85	2.53	3.23	**3.60**	0.31	0.12	0.10
SSA - 4M - 3/2 - 1.2	4.37	3.67	**4.80**	0.06	0.15	0.26
SSA - 6M - 3/2 - 1.2	**4.63**	4.23	3.67	0.12	0.21	0.29
SSA - 8M - 3/2 - 1.2	4.97	5.10	**5.80**	0.32	0.00	0.44
SSA - 10M - 3/2 - 1.2	5.80	5.20	**6.30**	0.44	0.30	0.20
80SSA20GBFS - 4M	3.23	3.70	**4.37**	0.06	0.17	0.61
80SSA20GBFS - 6M	3.10	3.37	**3.97**	0.10	0.31	0.45
80SSA20GBFS - 8M	3.73	4.17	**4.50**	0.15	0.35	0.79
80SSA20GBFS - 10M	4.07	**4.97**	4.03	0.15	0.40	0.15
50SSA50GBFS - 4M	22.93	27.47	**29.13**	2.60	1.88	7.63
50SSA50GBFS - 6M	**28.97**	25.60	28.23	1.37	1.13	2.51
50SSA50GBFS - 8M	**33.50**	26.17	31.03	4.53	0.21	3.12
50SSA50GBFS - 10M	**33.20**	31.70	29.07	4.36	0.87	5.67
25SSA75PC	26.83	26.90	**31.23**	2.91	0.10	1.50
50SSA50PC	21.03	18.80	**21.90**	1.61	1.93	1.73
75SSA25PC	11.77	**13.83**	11.70	0.15	0.76	2.10

*The highest compressive strength of each mixture is in bold

Universidade da Beira Interior | Faculdade de Engenharia
Calçada Fonte do Lameiro
6201-001 Covilhã | PORTUGAL

Tel.: +351 275 329 722 | E-mail: deca@ubi.pt

www.ubi.pt

25/53

Figure 16. Compressive Strength Results.

Universidade da Beira Interior | Faculdade de Engenharia
Calçada Fonte do Lameiro
6201-001 Covilhã | PORTUGAL

Tel.: +351 275 329 722 | E-mail: deca@ubi.pt

www.ubi.pt
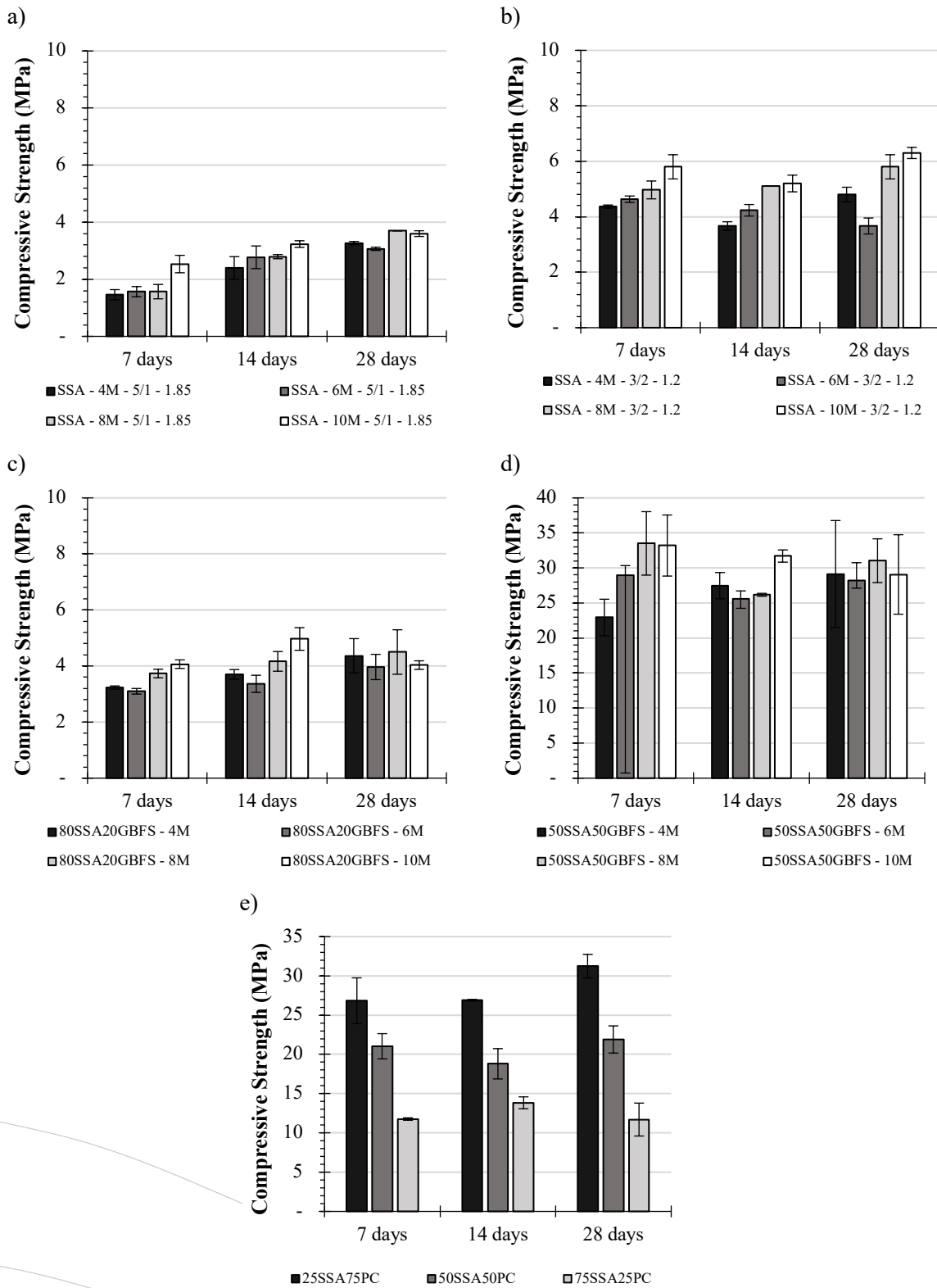
26/53

Mortars compositions of 50SSA50GBFS (8M and 10M) presented the highest compressive strength at 7 days. These mixtures also show no efflorescence. However, a reduction in compressive strength is verified at 14 and 28 days. The decrease in compressive strength might be related to the ratios of CaO/NaOH and PO_4/NaOH for the alkali-activated matrices tested in this study.

Regarding the standard deviation of the devised mortars, the mortars of 50SSA50GBFS present the highest standard deviation, although they present the highest compressive strength among the mortars produced. Thus, these mortar mixtures exhibit lower homogeneity in terms of compressive strength.

Therefore, and based only on compressive strength results, the 50SSA50GBFS (4M) is considered the best choice compared with others. Although it does not show the highest compressive strength at 7 days, it increases with time up to 28 days. It might indicate that for 50SSA50GBFS (10M) matrixes, an N-A-S-H type geopolymer is formed where gel changes occur during curing time. While in the case of 50SSA50GBFS (4M) matrixes, an hybrid SAP and/or C-A-S-H geopolymer is formed, which densifies over time.

4.3 TG-DTG

Figures 17 to 20 show a TG-DTG mass loss curves for several SSA-AM mortar mixtures, namely mortars obtained with 100% SSA, a blend of 50%SSA and 50%GBFS. Figure 21 shows TG-DTG mass loss curves for the different combinations of SSA and PC.
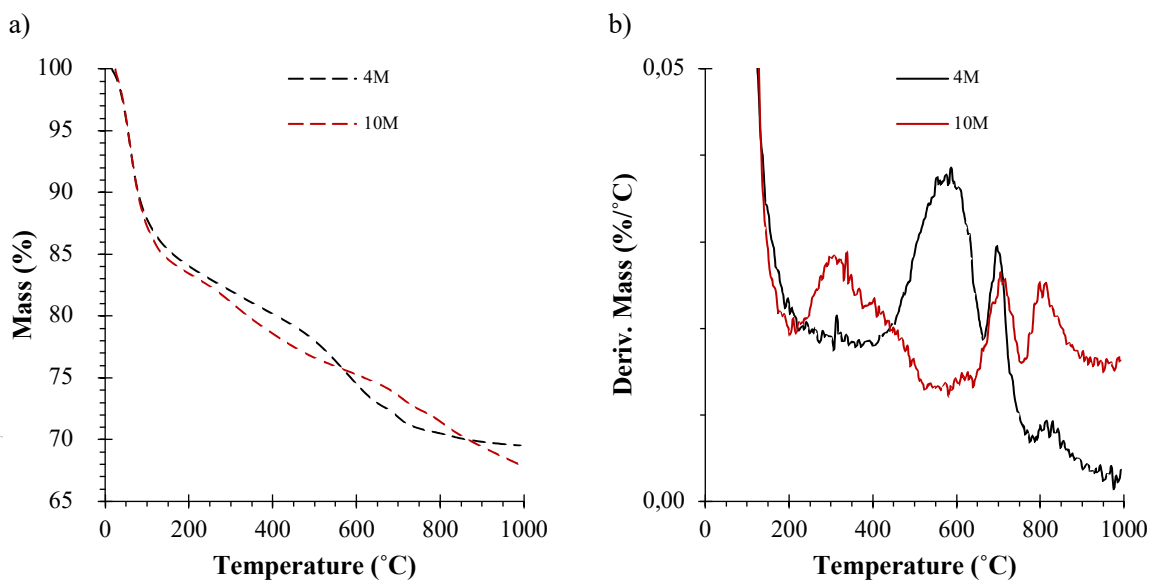
Figures 17 to 20 show a TG-DTG mass loss curves for several SSA-AM mortar mixtures, namely mortars obtained with 100% SSA, a blend of 50%SSA and 50%GBFS. Figure 21 shows TG-DTG mass loss curves for the different combinations of SSA and PC

Figure 17. (a) TG and (B) DTG curves of SSA - 4M - 5/1 - 1.85 and SSA - 10M - 5/1 - 1.85.

Universidade da Beira Interior | Faculdade de Engenharia
Calçada Fonte do Lameiro
6201-001 Covilhã | PORTUGAL

Tel.: +351 275 329 722 | E-mail: deca@ubi.pt
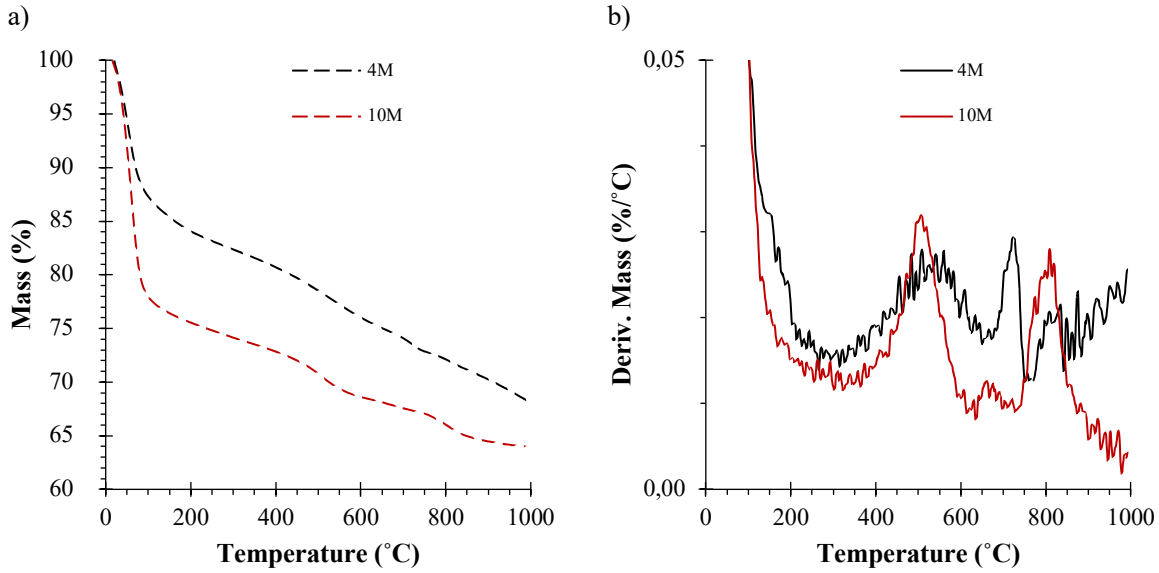
www.ubi.pt

27/53

Figure 18. (a) TG and (B) DTG curves of SSA - 4M - 3/2 - 1.20 and SSA - 10M - 3/2 - 1.20.
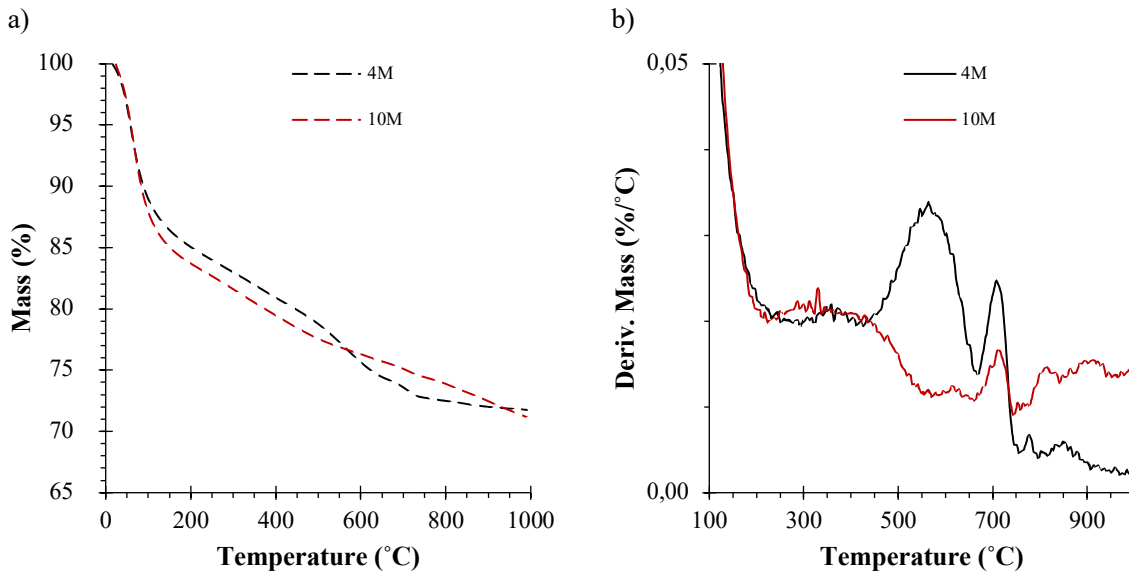
Figure 19. (a) TG and (B) DTG curves of 80SSA20GBFS - 4M and 80SSA20GBFS - 10M.
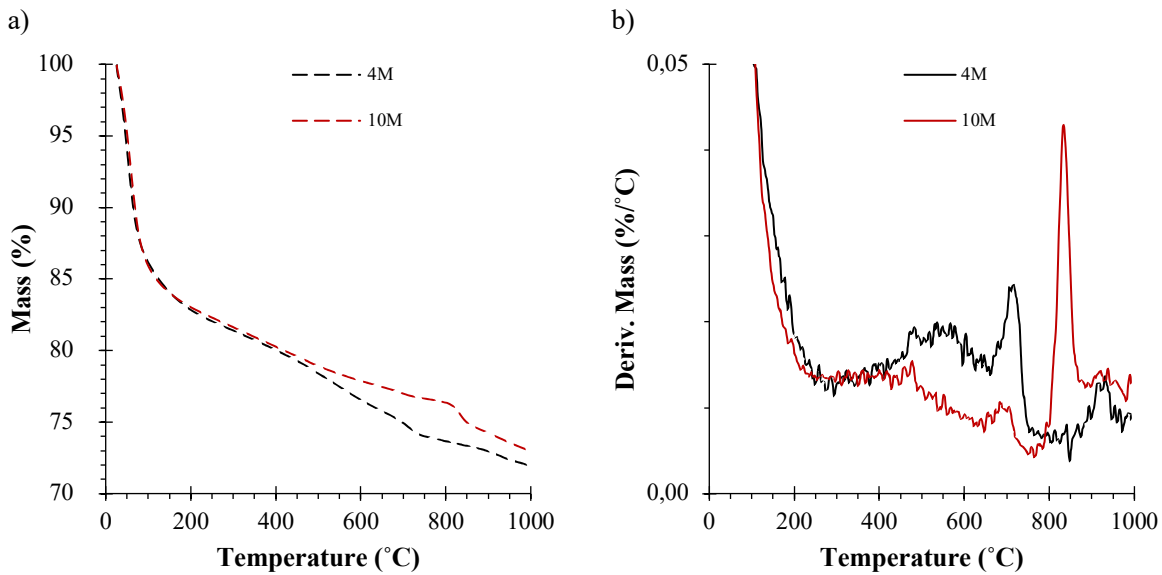
Universidade da Beira Interior | Faculdade de Engenharia
Calçada Fonte do Lameiro
6201-001 Covilhã | PORTUGAL

Tel.: +351 275 329 722 | E-mail: deca@ubi.pt

www.ubi.pt

28/53

a)

b)

Figure 20. (a) TG and (B) DTG curves of 50SSA50GBFS - 4M and 50SSA50GBFS - 10M.
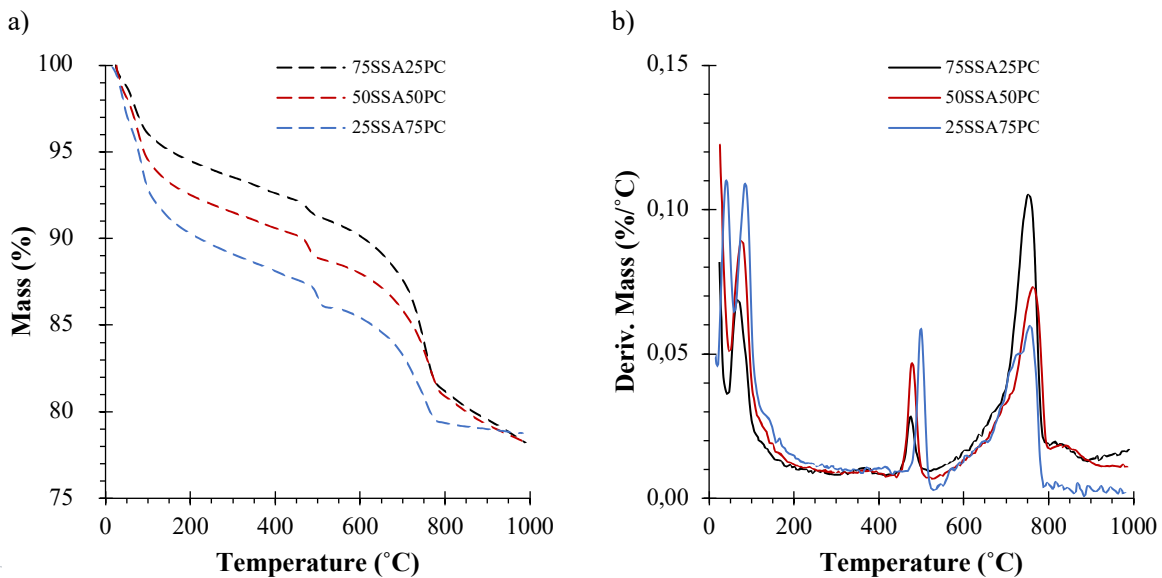
a)

b)

Figure 21. (a) TG and (B) DTG curves of 25SSA75PC, 50SSA50PC, and 75SSA25PC.

The TG-DTG mass loss follows two distinct trends regarding the liquid solution used. For water (PC mixtures), the mass loss is more evident in three temperature ranges, as expected (30 – 200 ˚C, 400-550 ºC and 600 – 800 ˚C). While for alkali solution, the mass loss is more

Universidade da Beira Interior | Faculdade de Engenharia
Calçada Fonte do Lameiro
6201-001 Covilhã | PORTUGAL

Tel.: +351 275 329 722 | E-mail: deca@ubi.pt

www.ubi.pt

29/53

evident in the temperature range of 30 – 200 ˚C, independently the mixture design as is exhibited in Table 7. Above 200 ºC, the weight loss is constant, and mass loss variation peaks are more diffuse (mass loss derivative), resulting in an overlapping of curves rather than well-defined peaks.

Table 7. Mass Loss (%) vs Temperature Range (˚C).

| Mixture Label | Mass Loss (%) - Temperature Range (˚C) | | | | | |
	30 – 200	200 – 400	400 – 600	600 – 800	800 – 980	Total
SSA - 4M - 1.85	**14.94**	3.87	5.66	4.01	0.95	29.42
SSA - 10M - 1.85	**15.79**	4.86	3.32	3.80	3.33	31.09
SSA - 4M - 1.2	**14.44**	3.35	4.67	3.91	3.59	29.96
SSA - 10M - 1.2	**22.43**	2.70	4.23	2.58	2.01	33.95
80SSA 20GBFS - 4M	**14.03**	4.13	5.26	3.16	0.70	27.28
80SSA 20GBFS - 10M	**15.66**	4.23	3.17	2.42	2.57	28.04
50SSA 50GBFS - 4M	**16.12**	2.81	3.46	2.92	1.54	26.85
50SSA 50GBFS - 10M	**16.23**	2.76	2.38	1.53	3.16	26.06
25SSA 75PC	**8.88**	2.17	2.67	6.10	0.57	20.39
50SSA 50PC	6.91	1.92	2.61	**7.10**	2.55	21.08
75SSA 25PC	5.05	1.86	2.47	**8.96**	2.82	21.17

Up to 200 ºC temperature, the weight loss (around 10%) correspond to changes in the chemical structure and the dehydration of free and chemically-bound water. Above 200 ºC, weight loss can also be attributed to removing adsorbed water molecules or differently linked in the hybrid alkaline binder phases. Those phases can be the dehydration of calcium silicate hydrate C-S-H gel, sodium alumino-silicate hydrates (N-A-S-H) and calcium alumino-silicate hydrates (C-A-S-H). It can also be attributed to poorly crystalline (sodium, calcium) alumino-silicate hydrates (N, C)-A-S-H and/or (sodium, potassium)-alumino-silicate hydrates (N, K)-A-S-H [4–6].

In particular, concerning 50SSA50GBFS (4M) and 50SSA50GBFS (10M) mixtures, the mass loss between 200 and up to 400 ºC is associated with amorphous and poorly crystalline hydrates. However, it is also possible that they are related to the decomposition of sound (N, C)-A-S-H and/or (N, K)-A-S-H gels. The weight loss between the temperature range of 400 to 600 ºC shows the continuous weight loss of the mixtures. Also, there is two sudden weight loss at around 650 ºC and 800 ºC. The first weight loss can be attributed to the decomposition of sound alkali-activated gels and the second (about 800 ºC) to the decomposition of calcite (CaCO$_3$). Thus, in the temperature range of 400 to 600 ºC, the weight loss response for the 50SSA50GBFS (4M) mixture shows that a more significant amount of cristaline sound alkali-activated gels was formed in comparison to the 50SSA50GBFS (10M) mixture. Besides, the blended mixture produced using a NaOH 10M concentration shows a higher peak corresponding to the decomposition of calcite (CaCO$_3$) (i.e., non-reacted calcite). Hence, part of the calcite content in the raw materials (50% SSA and 50% GGBFS) remains as an unreacted component and supports the results obtained by compressive strength testing (i.e., 50SSA50GBFS (10M) matrixes might be mainly formed by N-A-S-H type geopolymer where gel changes occur during time. While in the case of 50SSA50GBFS (4M), matrixes are developed by a hybrid SAP and/or C-A-S-H geopolymer, which densifies over time.

Universidade da Beira Interior | Faculdade de Engenharia
Calçada Fonte do Lameiro
6201-001 Covilhã | PORTUGAL

Tel.: +351 275 329 722 | E-mail: deca@ubi.pt

www.ubi.pt

30/53

As for Portland Cement TG-DTG, the temperature range between 400 and 600 ºC could be attributable to the thermal decomposition of calcium alumino-silicate hydrate (C-A-S-H)[7].

Moreover, the peaks located near the temperatures range 450-550 ºC corresponds to calcium hydroxide and between 600–800 ºC corresponds to the decomposition of calcite. Hence, it is also evident that higher calcite content in the raw materials (50% SSA and 50% GGBFS) remains an unreacted component for lower Portland cement content.

4.4   FT-IR

Figure 22 illustrates the FTIR spectra of all mortar specimens. The absorption bands at 667–797 cm-1 are due to Si-O-Si symmetrical stretching vibrations, which can be associated with quartz in the raw materials. Also, the peaks at 815 cm-1 typical for calcium carbonate phases (the out-of-plane bending of the C-O bond) can be seen in the raw materials, which is believed to correspond to calcite. Moreover, the broadening of the characteristic bands between 800 and 1200 cm-1 implies the overlap of more bands with a higher intensity, which is attributed to the stretching vibrations T-O-T bonds (where T = tetrahedral Si or Al), that confirms the presence of the alumino-silicate phases. Specifically, the peaks at 952 cm^{-1} are assigned to the Si-O stretching vibrations of SiO4 tetrahedron generated by Q2 tetrahedra that comprise C-S-H and, more specifically, C-A-S-H gel in the mortar specimens. The weak peaks at wavenumber 1252 cm^{-1} are attributed to the length as well as the angle of the Si-O and Al-O bonds in the silicates, in this case being sodium alumino-silicate (N-A-S-H) and/or calcium alumino-silicate (C-A-S-H) and probably other XRD-amorphous silicate phases in the spectrum of mortars. Strong peaks centred at wavenumber 1380-1476 cm^{-1} are associated with the asymmetric stretching vibration of O-C-O bonds of carbonate groups which are suggested to have occurred due to atmospheric carbonatation and possibly calcite from the content of the unreacted particles in the raw materials. Besides, the vibration at wavenumber 1082 cm^{-1} corresponds to Si-O and Al-O [8].
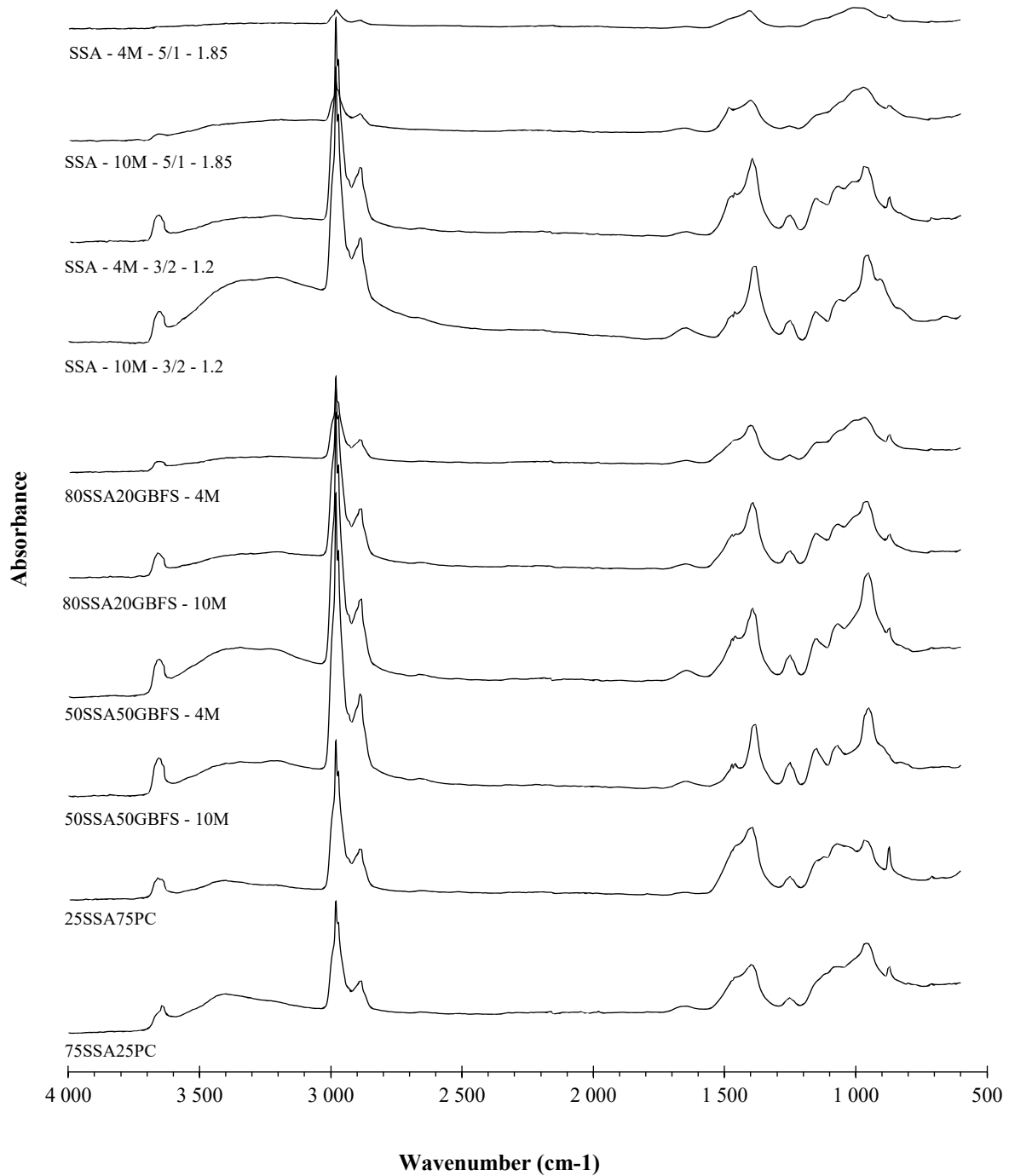
Universidade da Beira Interior | Faculdade de Engenharia
Calçada Fonte do Lameiro
6201-001 Covilhã | PORTUGAL

Tel.: +351 275 329 722 | E-mail: deca@ubi.pt

www.ubi.pt

31/53

Figure 22. FTIR absorbance of the devised mortars

Universidade da Beira Interior | Faculdade de Engenharia
Calçada Fonte do Lameiro
6201-001 Covilhã | PORTUGAL

Tel.: +351 275 329 722 | E-mail: deca@ubi.pt

www.ubi.pt

32/53
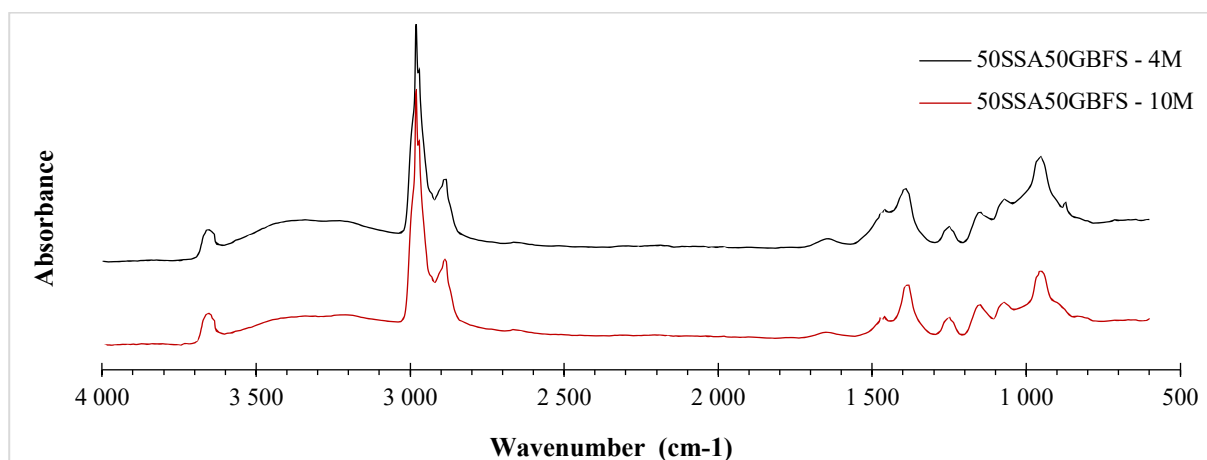
Figure 23. FTIR absorbance of the 50SSA50GBFS mortars

In all the mortar spectrums, the adsorption bands centred at 1624 cm-1 are due to the O-H bending of adsorbed H2O molecules. At the same time, the absorption bands at 3645 cm-1 indicate the presence of free O-H stretching vibration.

As for the FTIR spectra of the 50SSA50GBFS mortars in Figure 23 show some differences between the FTIR spectrum of the sample prepared with weak alkaline activator concentration (4M) to the one prepared with strong alkaline activator concentration (10M).

The absorbance increase in the 4M-based mortar spectrum indicates structural changes in the alkali-activation. More substantial absorbance at 950 cm^{-1} wavenumbers is noted, corresponding to a more significant quantity of the reaction products.

Mortar specimens synthesized from mixes prepared with weak alkali activator concentration (4M) present higher absorbances in the region of 1120-872 cm^{-1}. Such absorbance difference corresponds to the decreased quantity of Si-O-Al bonds (less N-A-S-H gel is formed) related to the lower Na/Ca ratio (4M-activated mixtures). On the other hand, more Si-O-Si bonds are formed (i.e., more C-A-S-H gel is created). Thus, for 4M-activated mixtures, larger quantities of reaction products, namely C-A-S-H gel, were produced. Therefore, this follows the compressive testing results.

4.5   SEM-EDS

The SEM images and EDS analysis over selected spots of the 28 days cured SSA-based alkali-activated mortar samples are shown in Figures 25-32. While the SEM images and EDS analysis over designated spots of the 28 days cured for SSA-PC mortar samples are shown in Figures 33 and 34.

4.5.1   Microstructure analysis of the SSA-based alkali-activated mortars

The morphology and microstructural characteristics of the SSA-based alkali-activated mortars specimens were studied under a scanning electron microscope (SEM) at 28 days. The

Universidade da Beira Interior | Faculdade de Engenharia
Calçada Fonte do Lameiro
6201-001 Covilhã | PORTUGAL

Tel.: +351 275 329 722 | E-mail: deca@ubi.pt

www.ubi.pt

33/53

reaction products/elemental compositions were determined using EDS analysis are shown in figures 24-33. The effect of the alkali activators concentration and the different L/S ratios are discussed below to relate their influence on the microstructure properties of the SSA-based alkali-activated mortars.

Figure 24 and Figure 25 shows the SEM images of the sample prepared with 100% SSA as a precursor and L/S= 1.85. Figure 26 and Figure 27 show the sample prepared with NaOH 4M and 10M, respectively. The morphology of the SSA-based alkali-activated mortar sample appears to be denser with a smaller number of pores. The SSA and sand particles are embedded in the matrix of the SSA-based alkali-activated mortar prepared with activator concentration 4 Mole.

The EDS spots of the sample prepared with NaOH 4M show lower Na content than the sample prepared with NaOH 10M. The Ca/Na ratio decreased in the samples by increasing the alkali activator concentration in the mixes.
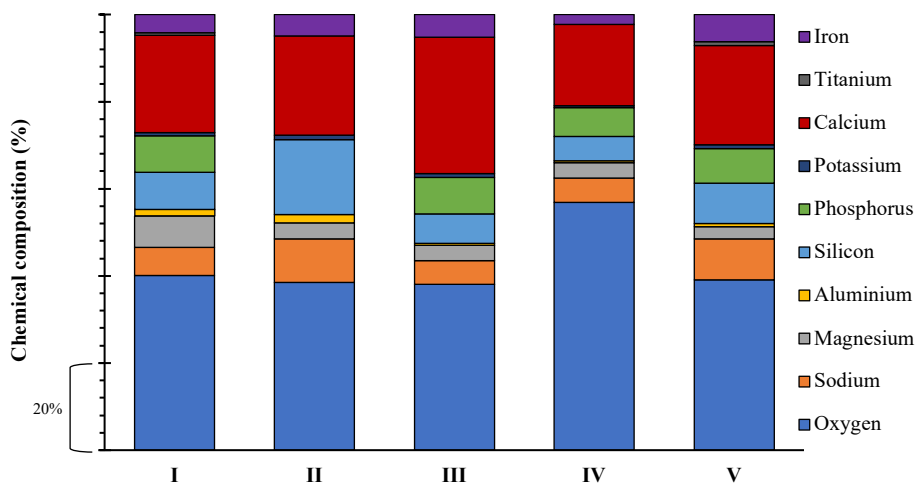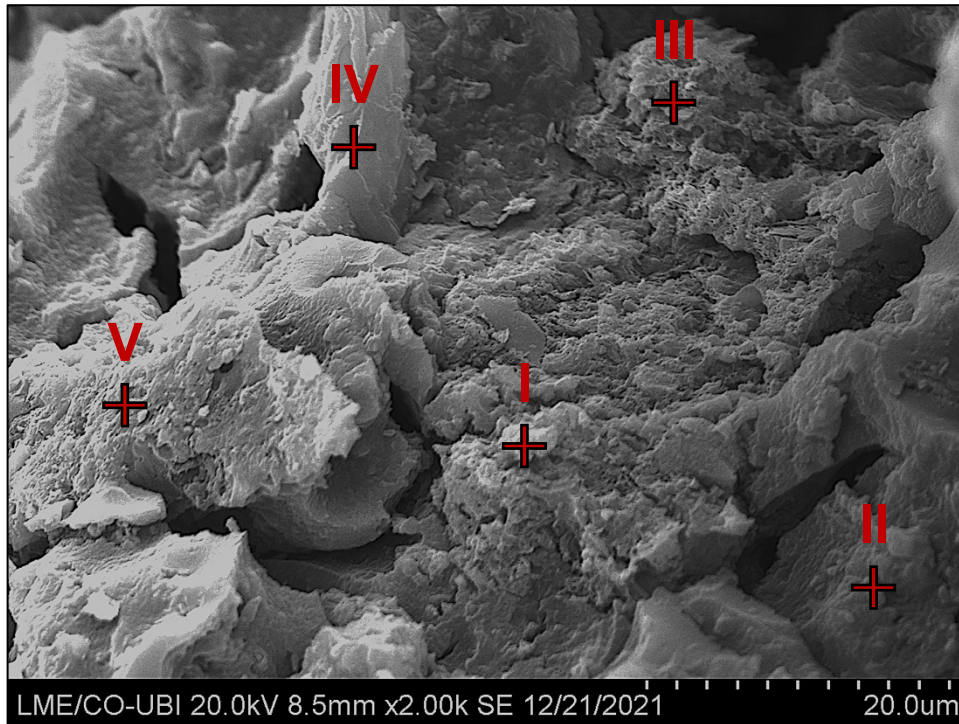
Universidade da Beira Interior | Faculdade de Engenharia
Calçada Fonte do Lameiro
6201-001 Covilhã | PORTUGAL

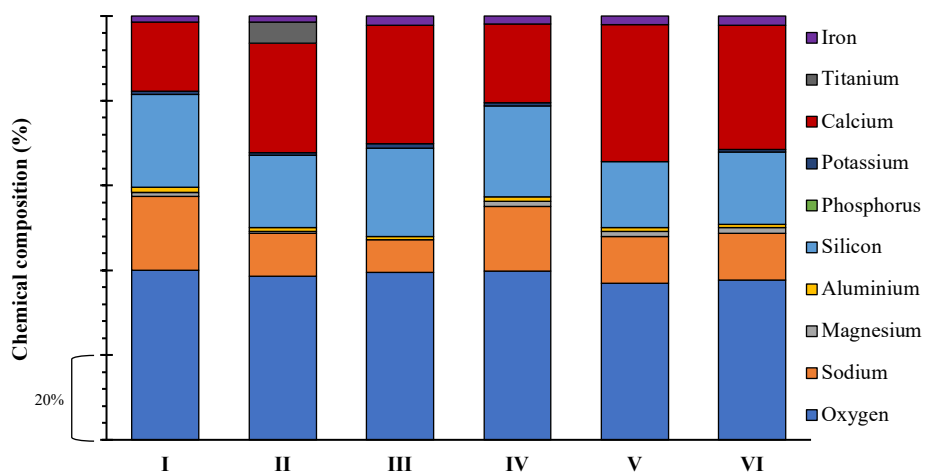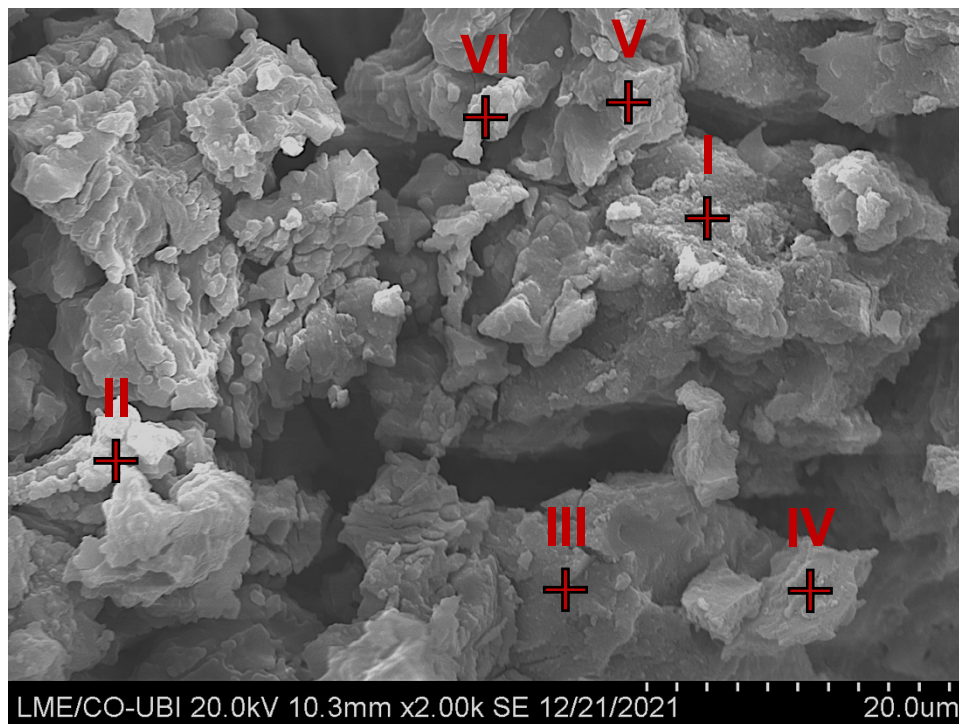Tel.: +351 275 329 722 | E-mail: deca@ubi.pt

www.ubi.pt

34/53

Figure 24. SEM image of SSA - 4M - 1.85.

Table 8. Elemental ratio of each spot of SSA - 4M - 1.85.

Elemental Ratio	I	II	III	IV	V
Ca/Na	3.47	2.28	5.84	3.35	2.43
Ca/Si	2.61	1.31	4.70	3.29	2.45
Na/Si	0.75	0.58	0.80	0.98	1.01
P/Na	1.29	-	1.59	1.18	0.85

Universidade da Beira Interior | Faculdade de Engenharia
Calçada Fonte do Lameiro
6201-001 Covilhã | PORTUGAL

Tel.: +351 275 329 722 | E-mail: deca@ubi.pt

www.ubi.pt

35/53

Figure 25. SEM image of SSA - 10M - 1.85.

Table 9. Elemental ratio of each spot of SSA - 10M - 1.85.

Elemental Ratio	I	II	III	IV	V	VI
Ca/Na	0.94	2.53	3.62	1.23	2.91	2.64
Ca/Si	0.74	1.51	1.33	0.87	2.08	1.72
Na/Si	0.79	0.60	0.37	0.71	0.71	0.65
P/Na	-	-	-	-	-	-

Universidade da Beira Interior | Faculdade de Engenharia
Calçada Fonte do Lameiro
6201-001 Covilhã | PORTUGAL

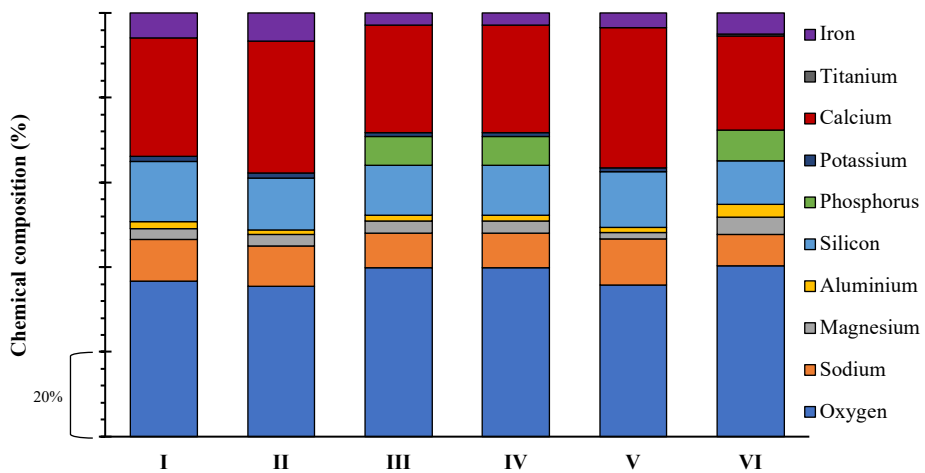Tel.: +351 275 329 722 | E-mail: deca@ubi.pt

www.ubi.pt

36/53
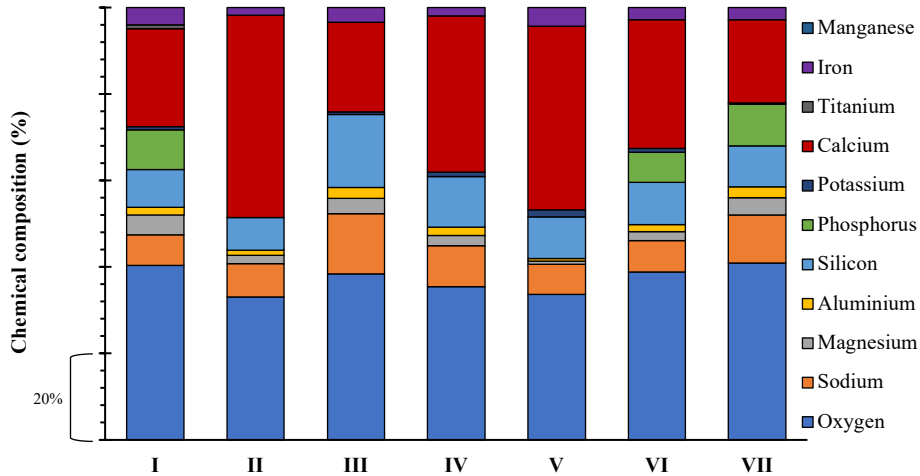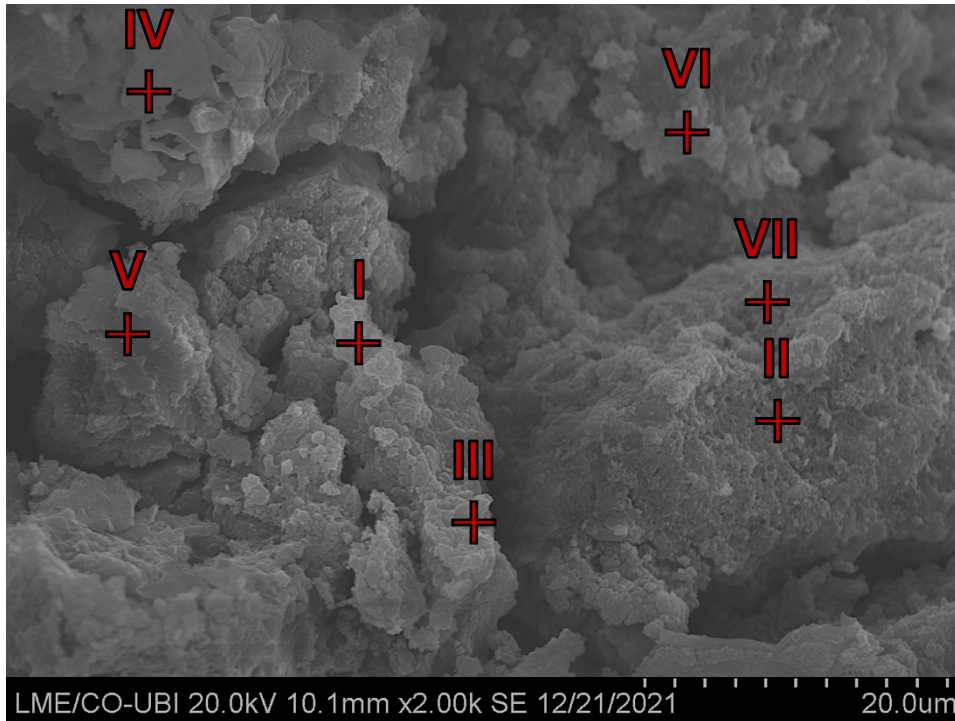
Figure 26. SEM image of SSA - 4M - 1.2.

Table 10. Elemental ratio of each spot of SSA - 4M - 1.2.

Elemental Ratio	I	II	III	IV	V	VI	VII
Ca/Na	3.22	6.12	1.49	3.78	6.11	4.08	1.72
Ca/Si	2.58	6.11	1.24	3.08	4.41	3.05	2.04
Na/Si	0.80	1.00	0.83	0.81	0.72	0.75	1.19
P/Na	1.29	-	-	-	-	0.95	0.86

Universidade da Beira Interior | Faculdade de Engenharia
Calçada Fonte do Lameiro
6201-001 Covilhã | PORTUGAL

Tel.: +351 275 329 722 | E-mail: deca@ubi.pt

www.ubi.pt

37/53
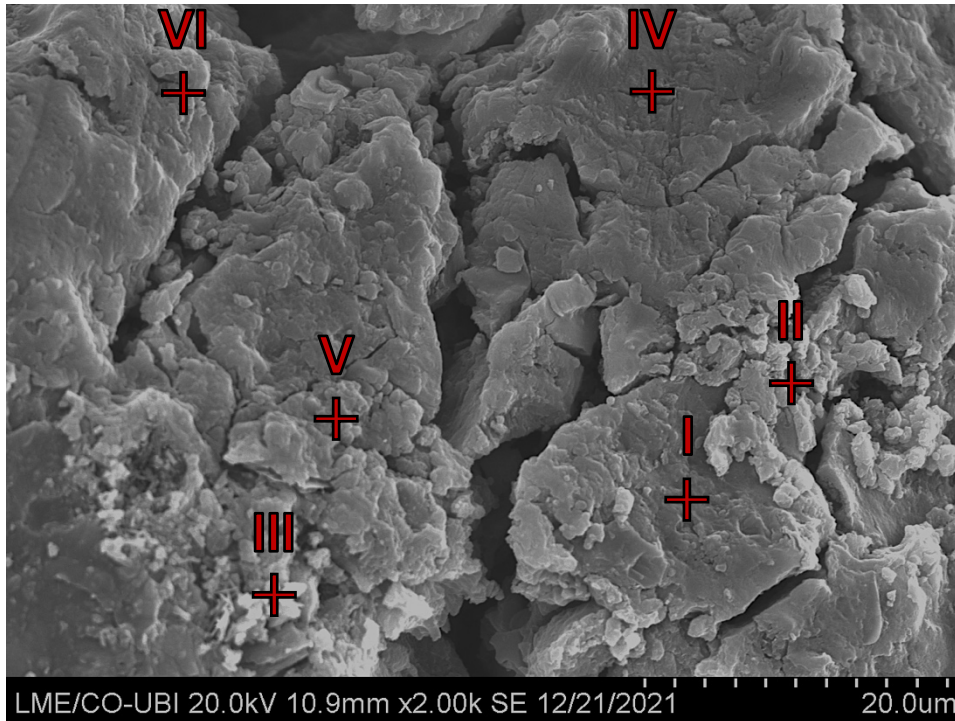
Figure 27. SEM image of SSA - 10M - 1.2.

Table 11. Elemental ratio of each spot of SSA - 10M - 1.2.

Elemental Ratio	I	II	III	IV	V	VI
Ca/Na	2.84	3.28	3.10	3.10	3.02	2.99
Ca/Si	1.97	2.55	2.17	2.17	2.53	2.17
Na/Si	0.69	0.78	0.70	0.70	0.84	0.73
P/Na	-	-	0.84	0.84	-	0.96

Universidade da Beira Interior | Faculdade de Engenharia
Calçada Fonte do Lameiro
6201-001 Covilhã | PORTUGAL

Tel.: +351 275 329 722 | E-mail: deca@ubi.pt

www.ubi.pt

38/53

4.5.2 Microstructure analysis of the SSA-GBFS based alkali-activated mortars

Figure 33 and Figure 34 shows the SEM images of the 50SSA50GBFS mortar samples prepared with a lower NaOH activator concentration (4M) and higher NaOH activator concentration (10M) respectively. The SEM images show an essential structure with a compact and homogeneous morphology.

Some spongy particles are observed in the mortar samples. More spongy products are formed in the sample prepared with a strong activator (10M) compared with those prepared with a weak (4M). These porous particles are considered hydrate (C2ASH8). Meanwhile, the alkali-activation reaction products generated in the mortar specimens are very complex, comprising a mix of different cementitious gels. It could not be asserted whether in these mixtures, an N-A-S-H, C-A-S-H phases or one highly crosslinked hybrid (C, M)-A-S-H gels where M = K, Na existed based only on the EDS microanalysis results.

The EDS spots of the sample prepared with NaOH 4M show lower Na content than the sample prepared with NaOH 10M. While the EDS spots of the sample prepared with NaOH 4M show higher Ca content than the sample prepared with NaOH 10M.

Higher Ca/Na ratio was observed in the 50SSA50GBFS sample prepared with a lower alkali activator (4M) concentration. The Ca/Na ratio decreased in the 50SSA50GBFS samples prepared with higher alkali activator concentration (10M).
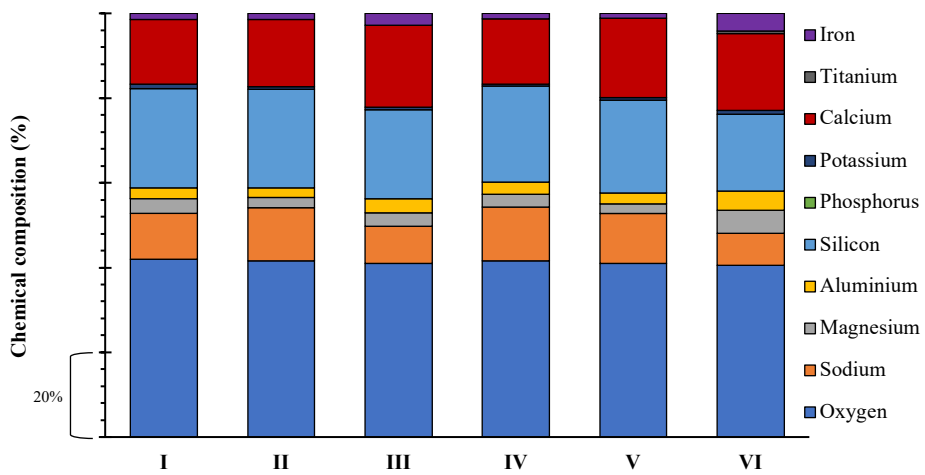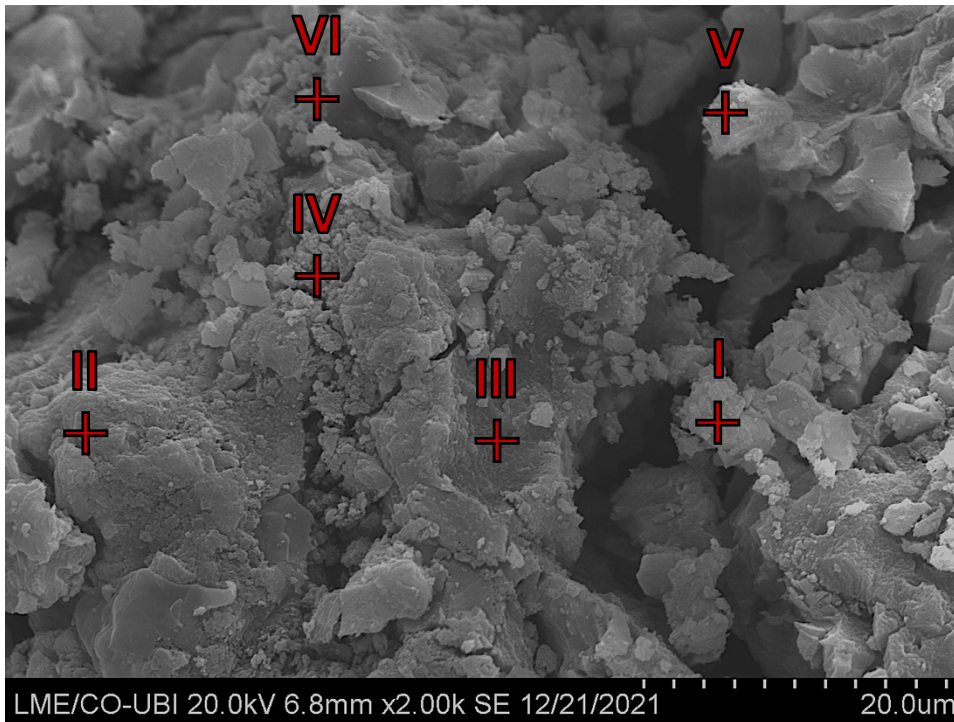
Universidade da Beira Interior | Faculdade de Engenharia
Calçada Fonte do Lameiro
6201-001 Covilhã | PORTUGAL

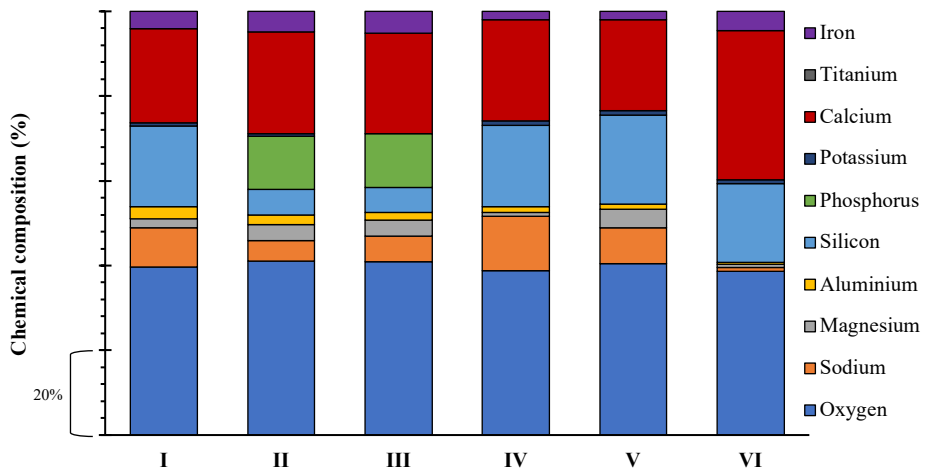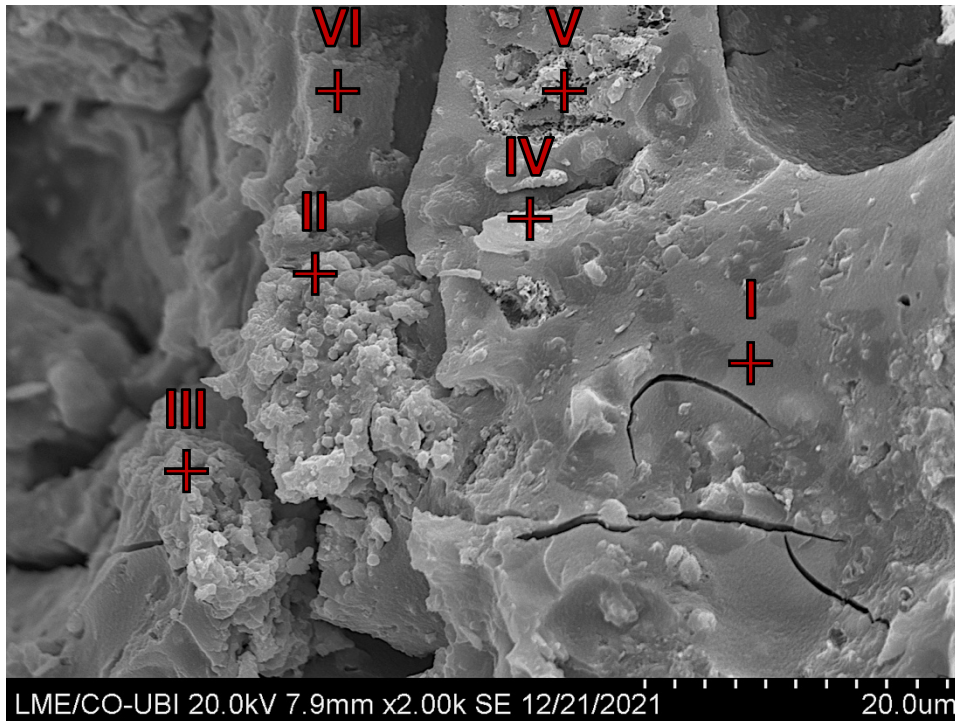Tel.: +351 275 329 722 | E-mail: deca@ubi.pt

www.ubi.pt

39/53

Figure 28. SEM image of 80SSA 20GBFS - 4M.

Table 12. Elemental ratio of each spot of 80SSA 20GBFS - 4M.

Elemental Ratio	I	II	III	IV	V	VI
Ca/Na	1.40	1.26	2.22	1.21	1.59	2.44
Ca/Si	0.65	0.68	0.92	0.67	0.85	1.00
Na/Si	0.46	0.54	0.41	0.55	0.53	0.41
P/Na	-	-	-	-	-	-

Figure 29. SEM image of 80SSA 20GBFS - 10M.

Table 13. Elemental ratio of each spot of 80SSA 20GBFS - 10M.

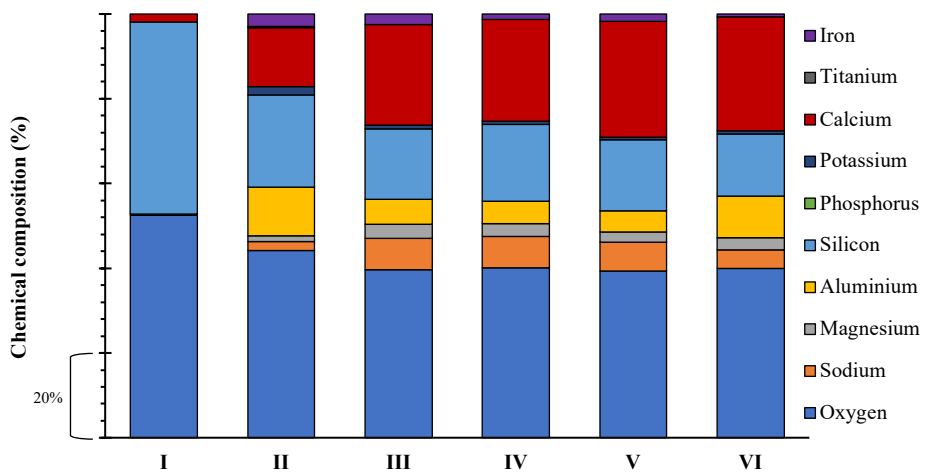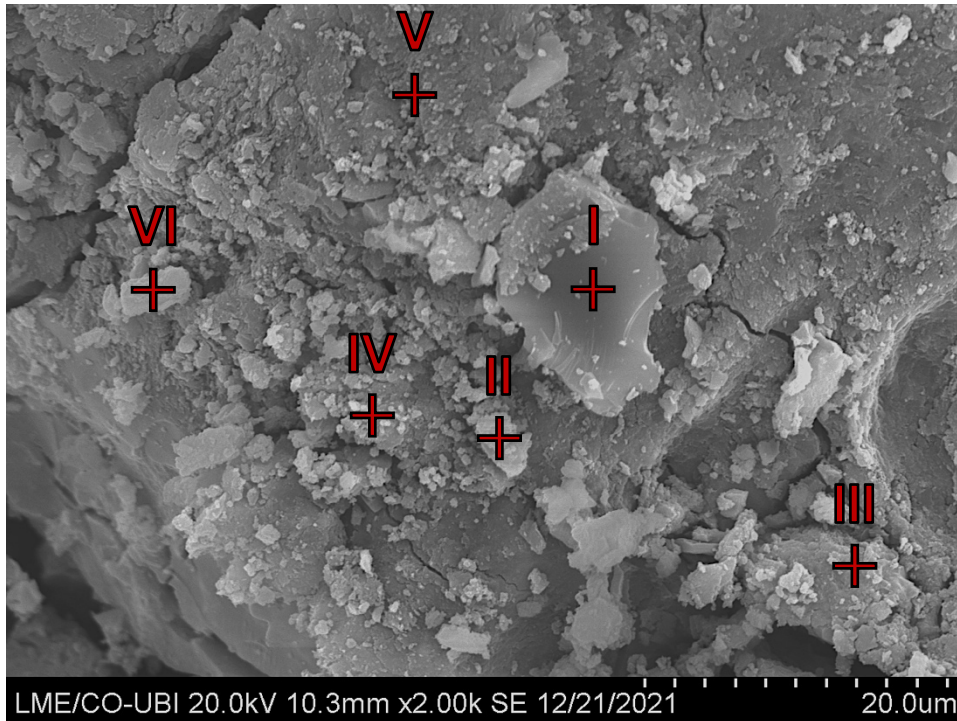| Elemental Ratio	I	II	III	IV	V	VI
Ca/Na	2.40	5.06	4.00	1.85	2.56	42.37
Ca/Si	1.16	3.98	4.06	1.24	1.02	1.88
Na/Si	0.48	0.79	1.02	0.67	0.40	0.04
P/Na	-	2.66	2.15	-	-	-

Figure 30. SEM image of 50SSA 50GBFS - 4M.

Table 14. Elemental ratio of each spot of 50SSA 50GBFS - 4M.

Elemental Ratio	I	II	III	IV	V	VI
Ca/Na	4.95	6.31	3.19	3.25	3.98	6.11
Ca/Si	0.04	0.64	1.42	1.33	1.63	1.85
Na/Si	0.01	0.10	0.45	0.41	0.41	0.30
P/Na	-	-	-	-	-	-

Universidade da Beira Interior | Faculdade de Engenharia
Calçada Fonte do Lameiro
6201-001 Covilhã | PORTUGAL

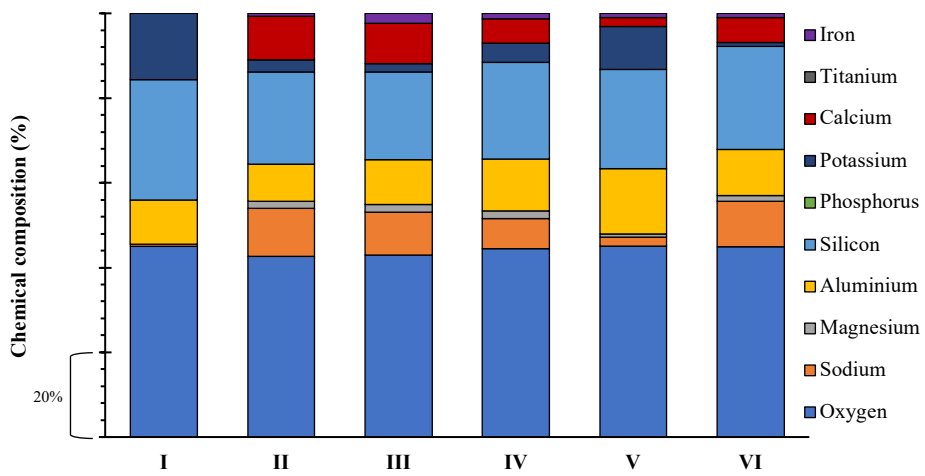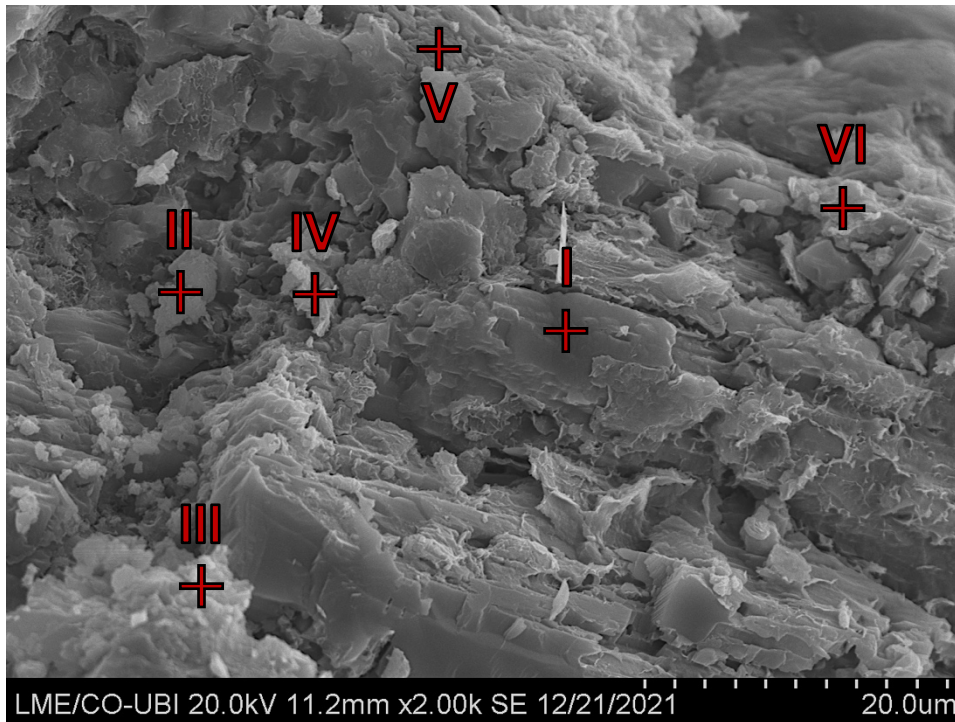Tel.: +351 275 329 722 | E-mail: deca@ubi.pt

www.ubi.pt

42/53

Figure 31. SEM image of 50SSA 50GBFS - 10M.

Table 15. Elemental ratio of each spot of 50SSA 50GBFS - 10M.

Elemental Ratio	I	II	III	IV	V	VI
Ca/Na	-	0.92	0.94	0.80	0.99	0.55
Ca/Si	-	0.48	0.46	0.25	0.09	0.24
Na/Si	0.02	0.52	0.49	0.31	0.09	0.44
P/Na	-	-	-	-	-	-

4.5.3   Microstructure of the SSA-Portland cement blended mixtures

In this study, different dosages of SSA (25, 50 and 75 wt.%) were added to the Portland cement to prepare mortars. In Figs 32 and 33 are re shown the effect of the different SSA dosages on the microstructure of the prepared mortars.

The morphology of the 75PC+25 SSA sample appears to be denser with a smaller number of pores unreacted particles (SSA and PC) surrounded by crystals needles morphology. These needles correspond to the formation of Ettringites. The sample exhibited a large number of needle-like crystals in the matrix areas.
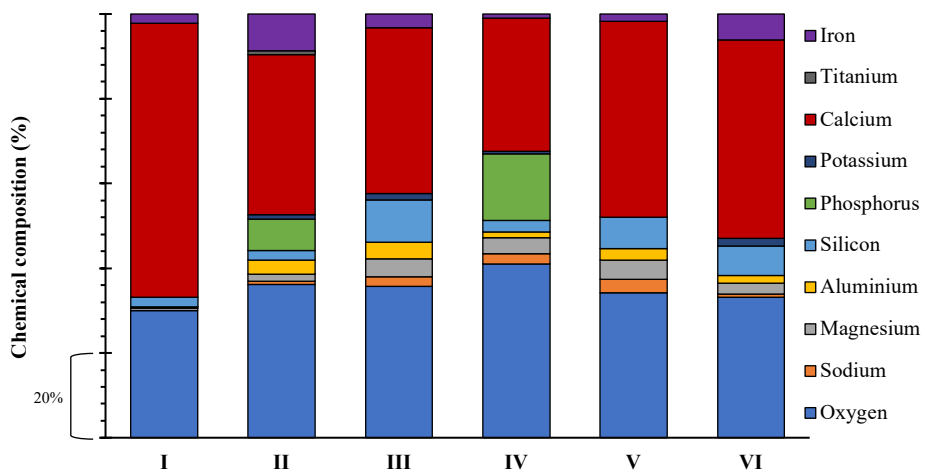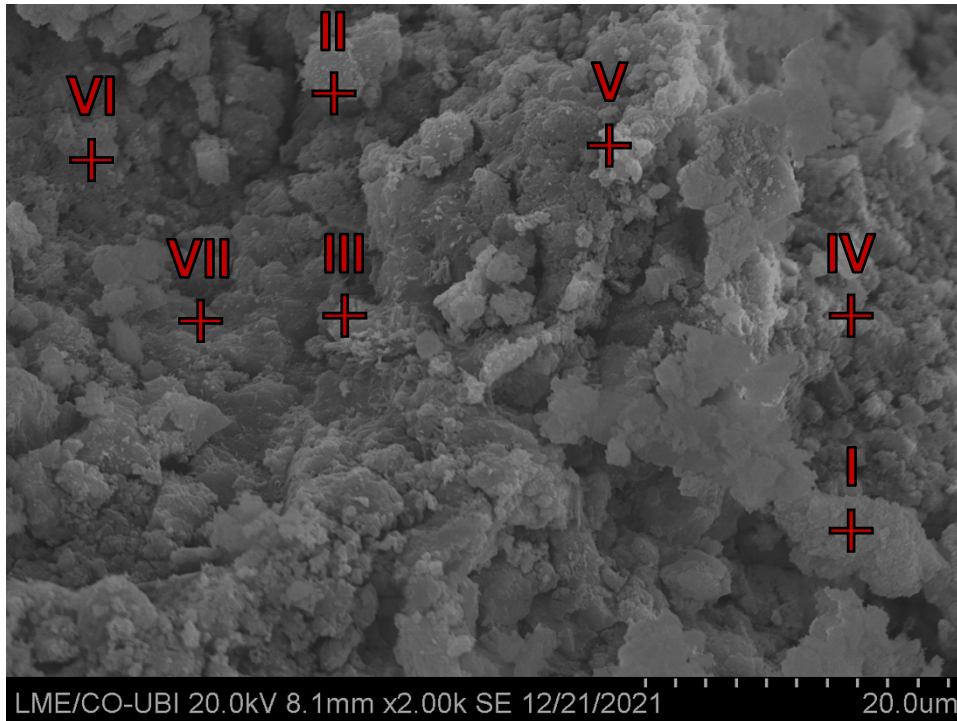
Universidade da Beira Interior | Faculdade de Engenharia
Calçada Fonte do Lameiro
6201-001 Covilhã | PORTUGAL

Tel.: +351 275 329 722 | E-mail: deca@ubi.pt

www.ubi.pt

44/53

Figure 32. SEM image of 75SSA 25PC.

Table 16. Elemental ratio of each spot of 75SSA 25PC.

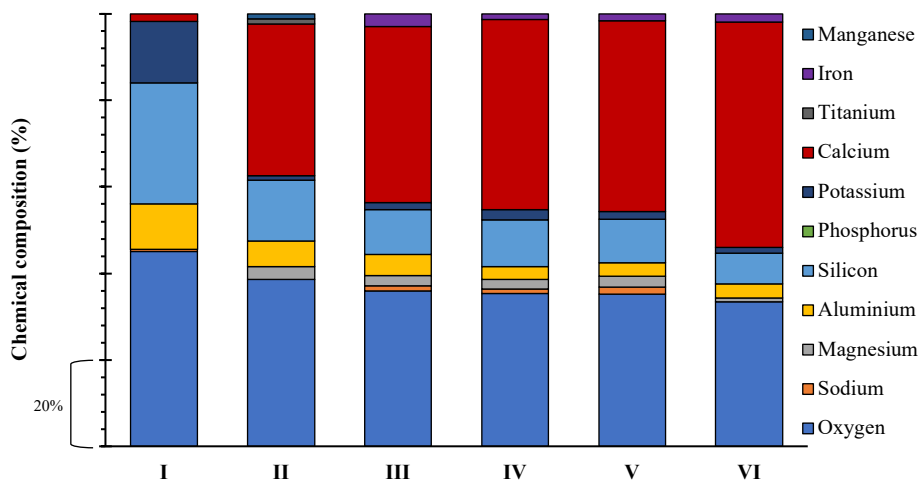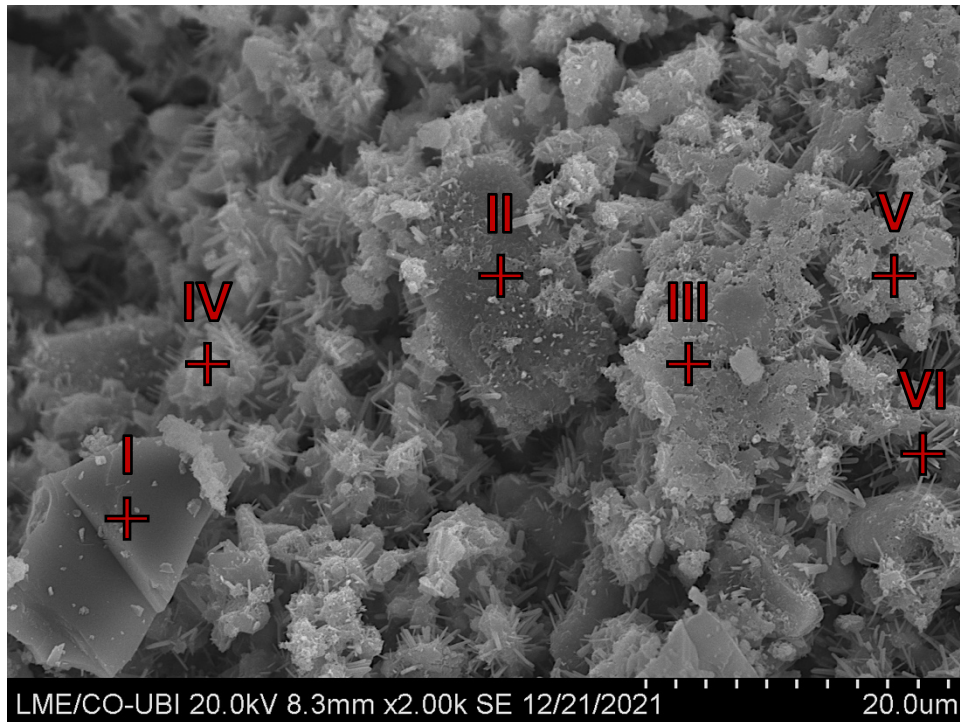| Elemental Ratio	I	II	III	IV	V	VI
Ca/Na	-	44.46	16.96	13.13	14.24	65.85
Ca/Si	28.85	16.08	3.91	11.33	6.18	6.74
Na/Si	-	0.36	0.23	0.86	0.43	0.10
P/Na	-	8.78	-	6.58	-	-

Figure 33. SEM image of 25SSA 75PC.

Table 17. Elemental ratio of each spot of 25SSA 75PC.

Elemental Ratio	I	II	III	IV	V	VI
Ca/Na	3.32	-	35.12	41.18	27.77	-
Ca/Si	0.06	2.50	3.98	4.11	4.38	7.33
Na/Si	0.02	-	0.11	0.10	0.16	-
P/Na	-	-	-	-	-	-

Universidade da Beira Interior | Faculdade de Engenharia
Calçada Fonte do Lameiro
6201-001 Covilhã | PORTUGAL

Tel.: +351 275 329 722 | E-mail: deca@ubi.pt

www.ubi.pt

46/53

4.6 MIP

The MIP analysis's main results are presented in Table 18. The porosity of the devised mortars ranges from 18.05 to 38.13 %, depending on the mixture design and solution molarity. For mixtures embodying only SSA, the increase in molarity represents a decrease in porosity. On the other hand, for mixtures comprising SSA and GBFS, their porosity increases when used solutions with higher molarity. Besides, the porosity decreases as the content of PC increases in the mortar that hold PC and SSA as a binder agent.

Table 18. MIP results of the different mortars

Mixture	Porosity (%)	Bulk Density at 14.50 psia (g/mL)	Apparent (skeletal) Density (g/mL)	Average Pore Diameter (μm)	Critical pore diameter (μm)
SSA - 4M - 1.85	38.13	2.16	2.65	0.14	30.15
SSA - 10M - 1.85	32.28	2.33	2.66	0.14	40.16
SSA - 4M - 1.2	35.12	2.13	2.76	0.05	22.61
SSA - 10M - 1.2	29.45	2.28	2.72	0.20	30.15
80SSA 20GBFS - 4M	30.95	2.07	2.62	0.06	15.75
80SSA 20GBFS - 10M	31.32	2.31	2.73	0.08	36.16
50SSA 50GBFS - 4M	18.05	2.26	2.64	0.03	0.01
50SSA 50GBFS - 10M	19.82	2.26	2.64	0.08	13.41
25SSA 75PC	19.03	2.23	2.72	0.05	1.05
75SSA 25PC	24.03	2.16	2.79	0.06	0.43

Such parameters range from 2.07 to 2.33 g/mL concerning the bulk density. The mixtures that used higher molarity solution present higher bulk density, and the mixture using more PC also show higher results. At the same time, the average pore diameter and critical diameter present higher values for mixtures with higher molarity solutions and more PC content. The critical diameter is represented by the maximum value of the Log differential intrusion axis in Figure 34.
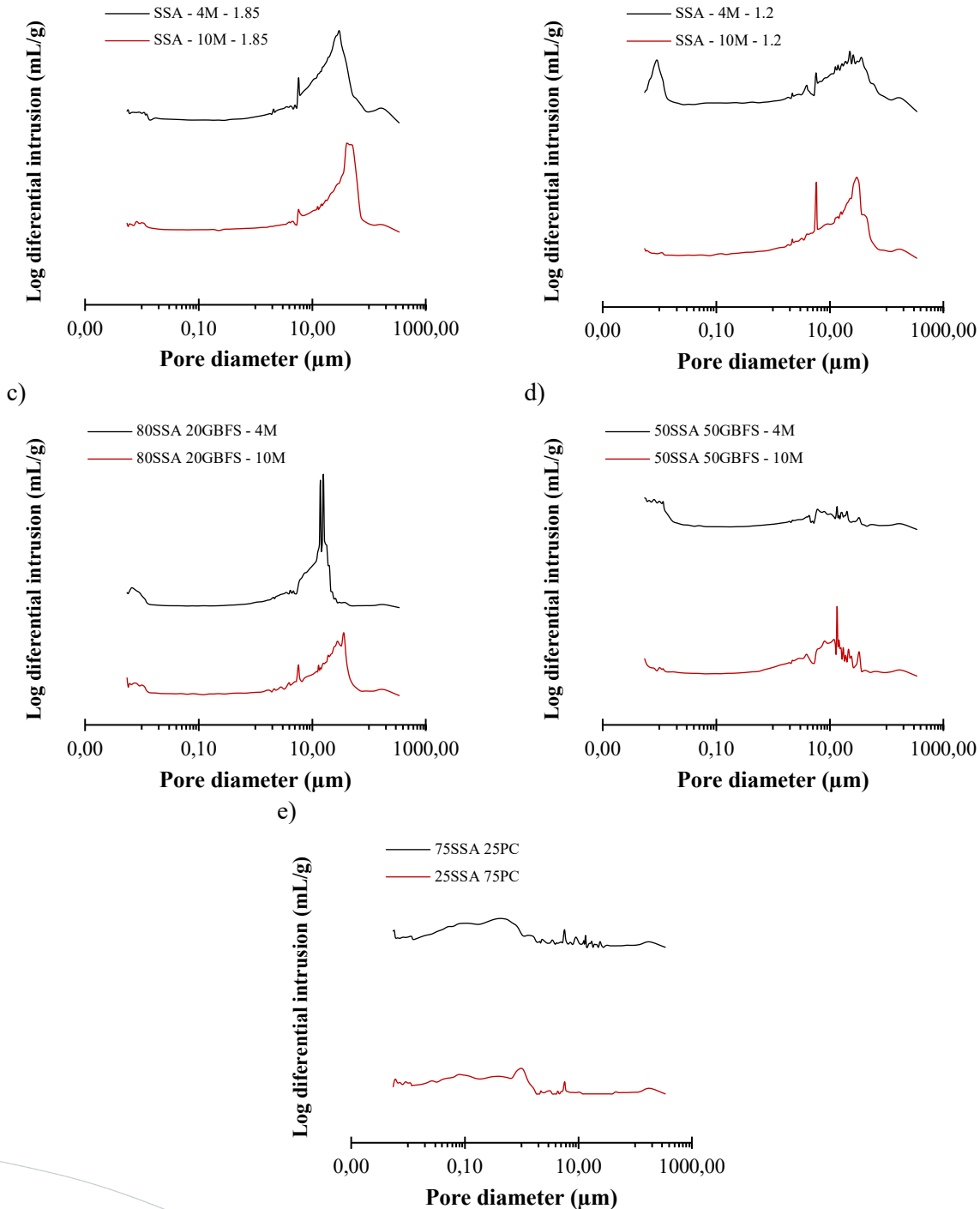
a)   b)

Universidade da Beira Interior | Faculdade de Engenharia
Calçada Fonte do Lameiro
6201-001 Covilhã | PORTUGAL

Tel.: +351 275 329 722 | E-mail: deca@ubi.pt

www.ubi.pt

47/53

c)

d)

e)

Figure 34. Log differential intrusion.

According to IUPAC [9], the dimension of the pore diameter (∅) of a cementitious matrix can be used to classify its pores in: (i) micropores (∅ ≤ 0.002 μm); (ii) mesopores (0.002 μm < ∅ ≤ 0.05 μm); (iii) macropores (0.05 μm < ∅ ≤ 10 μm); and (iv) air voids/cracks (∅ ≥ 10

Universidade da Beira Interior | Faculdade de Engenharia
Calçada Fonte do Lameiro
6201-001 Covilhã | PORTUGAL

Tel.: +351 275 329 722 | E-mail: deca@ubi.pt

www.ubi.pt

48/53

μm). Thus, Figure 35 displays the relationship curves between the cumulative mercury intrusion and the pore size. Based on these results, it was possible to determine the percentage of pores of each mixture in a certain diameter range, as shown in Table 19 and visualized in Figure 36.
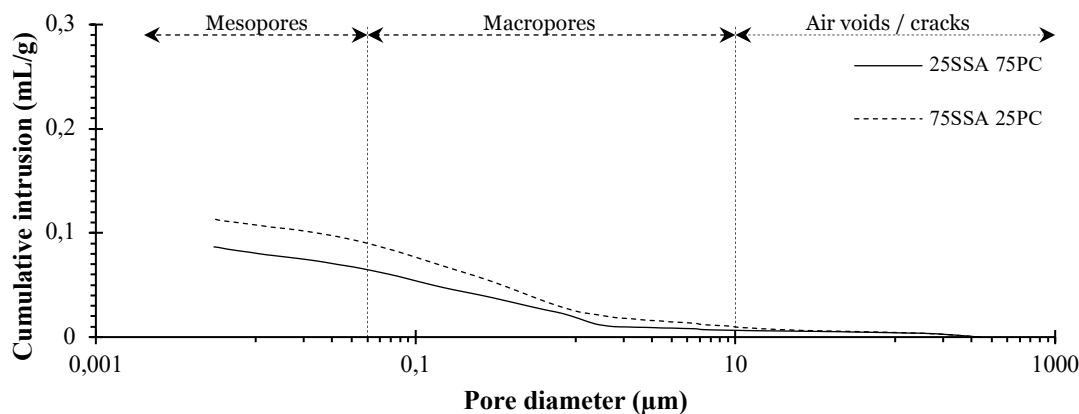
a)
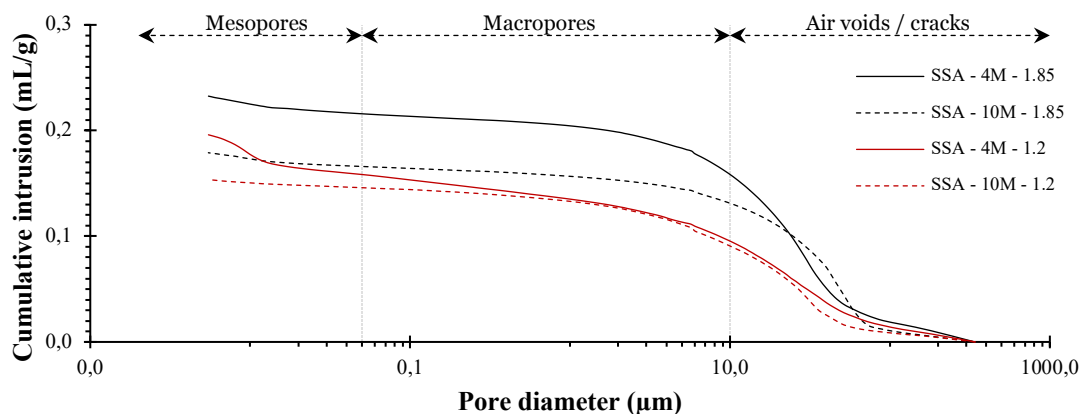
b)
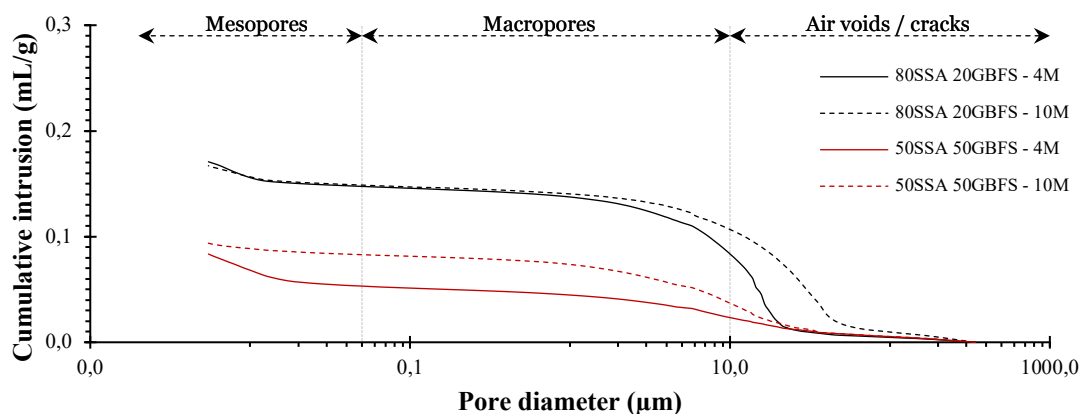
c)

Figure 35. Pores size distribution curves of the different mortars

Table 19. Pores size distribution of the different mortars

Mixture	Pores typology (%) [9]		
	Mesopores	Macropores	Air voids/cracks
SSA - 4M - 1.85	7.20	25.61	**67.20**
SSA - 10M - 1.85	7.26	20.03	**72.71**
SSA - 4M - 1.2	19.19	32.86	**47.95**
SSA - 10M - 1.2	5.07	36.88	**58.06**
80SSA 20GBFS - 4M	13.67	39.12	**47.21**
80SSA 20GBFS - 10M	10.94	26.02	**63.04**
50SSA 50GBFS - 4M	36.34	**36.42**	27.24
50SSA 50GBFS - 10M	11.58	**50.47**	37.95
75SSA 25PC	20.65	**71.15**	8.21
25SSA 75PC	25.37	**67.20**	7.43

In bold the predominant pore typology

a)
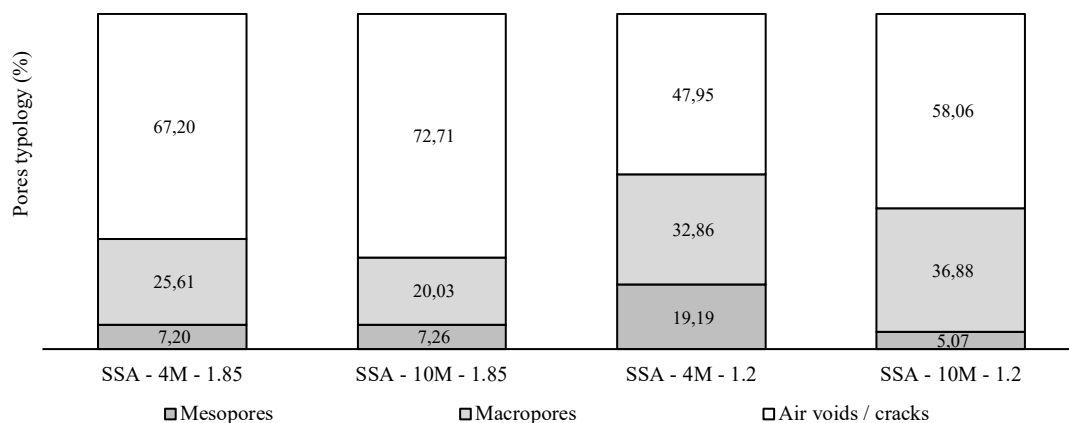
b)
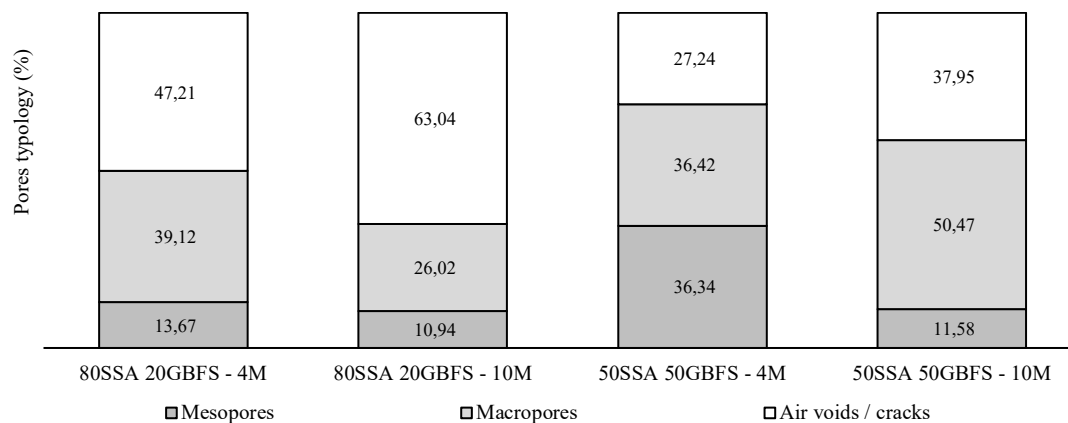
c)

Figure 36. Pores typology.

The presence of macropores is predominant in those mixtures containing PC and 50% of GBFS. Thus, the results show a higher level of mesopores for the mixture comprising 50% of GBFS and solution molarity of 4M, for mixtures containing PC, and for SSA-4M-1.2.

Finally, air void/crack is dominant in those mixtures that use only SSA and those that embody 20% of GBFS as SSA replacement. Therefore, these results correlate with the compressive strength results since the high air void/crack volume led to reduced compressive strength results. In contrast, the sum of macropores and mesopores volume led to higher compressive strength results, mainly observed in those mixtures containing PC and at those where SSA was replaced by 50% by GBFS.

Universidade da Beira Interior | Faculdade de Engenharia
Calçada Fonte do Lameiro
6201-001 Covilhã | PORTUGAL

Tel.: +351 275 329 722 | E-mail: deca@ubi.pt

www.ubi.pt

51/53

5   Conclusions

The feasibility for alkali-activation of a Sewage Sludge Ash (SSA) supplied from a local municipality was carried on. The study comprised lower and higher NaOH alkali-activation and Portland cement hydration.

The preliminary study was carried on using SSA, glass waste (GW), grounded blast furnace slag (GBFS) and sand (mortar mixtures). It aimed at studying the setting time, workability (Spread test) and efflorescence phenomena. 28 different mortar mixtures were prepared using a small amount of material (about 50 cm^3). Specimens were produced with both sodium silicate and NaOH at different Molar concentrations. This study found that many factors may exert influence on the alkali-activated mortars (SSA-AAM) due to the SSA complex chemical composition, as well as: (i) type of the alkali-activator solution; (ii) molarity of NaOH solution; (iii) ratios (NaOH/sodium silicate and Solid/ Liquid); and (iv) curing conditions. Therefore, the mixture labels suggested were SSA1.2-5/1-4-60˚C and SSA1.2-5/1-10-60˚C since these mixtures achieved normal setting time and good workability without presenting the efflorescence phenomena.

The mixtures design phase was followed using SSA, grounded blast furnace slag (GBFS) and sand (mortar mixtures). Besides, the mixtures design phase also aimed to obtain chemical activation (hydration) of SSA with Portland cement. In this phase, 19 mixtures were produced for a total volume of about 864 cm^3 each. Due to the size effect on the workability, the mixture designs were adapted. The mixtures design phase aimed at studying the compressive strength, TG-DTG, FTIR, SEM-EDS and MIP. Results obtained showed that mortars embodying SSA and GBFS (50SSA50GBFS) as binders presented better compressive strength when compared with others, namely, the one made of weak alkali-activation (4M NaOH). Presenting both progressive strength gain and the highest compressive strength at 28 days. As for TG-DTG, FITR and SEM-EDS analyses, they confirm the compressive strength behaviour. The TG-DTG test showed that a large amount of sound and crystalline alkali-activated gels might be formed in this mixture design.

The FTIR spectrum indicates that larger quantities of reaction products, namely C-A-S-H gels, were formed. SEM-EDS analyses revealed denser structure and evidence of both C-A-S-H and N-A-S-H gels formed and silico-aluminophosphate (SAP) gel traces. Finally, 50SSA50GBFS mortar made of weak alkali-activation (4M NaOH) presented the lowest porosity, average pore diameter and critical pore diameter.

Universidade da Beira Interior | Faculdade de Engenharia
Calçada Fonte do Lameiro
6201-001 Covilhã | PORTUGAL

Tel.: +351 275 329 722 | E-mail: deca@ubi.pt

www.ubi.pt

52/53

6 References

[1]   Y.S. Wang, Y. Alrefaei, J.G. Dai, Silico-aluminophosphate and alkali-aluminosilicate geopolymers: A comparative review, Front. Mater. 6 (2019) 1–17. https://doi.org/10.3389/fmats.2019.00106.

[2]   Y. Wang, Y. Alrefaei, J. Dai, Influence of coal fly ash on the early performance enhancement and formation mechanisms of silico-aluminophosphate geopolymer, Cem. Concr. Res. 127 (2020) 105932. https://doi.org/10.1016/j.cemconres.2019.105932.

[3]   R.O. Yusuf, Z.Z. Noor, M.F.M. d. Din, A.H. Abba, Use of sewage sludge ash (SSA) in the production of cement and concrete - A review, Int. J. Glob. Environ. Issues. 12 (2012) 214–228. https://doi.org/10.1504/IJGENVI.2012.049382.

[4]   X. Gao, Q.L. Yu, H.J.H. Brouwers, Reaction kinetics, gel character and strength of ambient temperature cured alkali-activated slag–fly ash blends, Constr. Build. Mater. 80 (2015) 105–115. https://doi.org/10.1016/j.conbuildmat.2015.01.065.

[5]   F. Škvára, L. Kopecký, V. Šmilauer, Z. Bittnar, Material and structural characterization of alkali activated low-calcium brown coal fly ash, J. Hazard. Mater. 168 (2009) 711–720. https://doi.org/10.1016/j.jhazmat.2009.02.089.

[6]   A. Trník, L. Scheinherrová, I. Medveď, R. Černý, Simultaneous DSC and TG analysis of high-performance concrete containing natural zeolite as a supplementary cementitious material, J. Therm. Anal. Calorim. 121 (2015) 67–73. https://doi.org/10.1007/s10973-015-4546-8.

[7]   S.A. Bernal, M.C.G. Juenger, X. Ke, W. Matthes, B. Lothenbach, N. De Belie, J.L. Provis, Characterization of supplementary cementitious materials by thermal analysis, Mater. Struct. Constr. 50 (2017) 1–13. https://doi.org/10.1617/s11527-016-0909-2.

[8]   Z. Sun, H. Cui, H. An, D. Tao, Y. Xu, J. Zhai, Q. Li, Synthesis and thermal behavior of geopolymer-type material from waste ceramic, Constr. Build. Mater. 49 (2013) 281–287. https://doi.org/10.1016/j.conbuildmat.2013.08.063.

[9]   D.H. Everett, Manual of Symbols and Terminology for Physicochemical Quantities and Units, Appendix II: Definitions, Terminology and Symbols in Colloid and Surface Chemistry, Pure Appl. Chem. 31 (1972) 577–638. https://doi.org/10.1351/pac197231040577.

Universidade da Beira Interior | Faculdade de Engenharia
Calçada Fonte do Lameiro
6201-001 Covilhã | PORTUGAL

Tel.: +351 275 329 722 | E-mail: deca@ubi.pt

www.ubi.pt

53/53